CHAPTER I

INTRODUCTION

1.0 GENERAL

Industry automation is mainly developed around motion control systems where the controlled electric motors play an important function in modern process automation. Therefore, the performance of an automated process largely depends on the high performance motor control system. The performance is defined in terms of accuracy, smooth operation and also on the simplicity of the controlling technique/scheme. The recent developments in the power electronic industry have resulted in the large improvements in the automation system for industrial processes. Recent advances in the development of fast semiconductor switches and cost-effective DSPs and micro-processors have opened a new era for the adjustable speed drive. These developments have helped the field of motor drives by shifting complicated hardware control structures onto software based advanced control algorithms. The result is a considerable improvement in cost while providing better performance of the overall drive system. In the present work, operation and controlled performance of Brushless DC motor in different modes of operation and effect of operating condition like sudden application of load, change of reference speed etc. is discussed in details.

1.1 DC AND AC MOTORS AND THEIR TRENDS

Unlike DC brush motor, Alternating current i.e. AC motors e.g. Synchronous and Induction Motors (IM) are more rugged and widely used in industries due to their lower weight, inertia and lower cost than DC motors. The main advantage of the AC motors over the DC motors is that there is no requirement of an electrical connection between the stationary part and rotating parts of the motor. Therefore, the AC motors do not need any mechanical commutator and brush assembly, resulting in lesser maintenance. They also have higher efficiency than DC motors and a high overload capability.

All of the advantages listed above justify that AC motors are more robust, cheap, and less prone to failure at high speeds. Furthermore, these can work in explosive and corrosive environments as these don’t produce sparks and thus is the perfect choice for

electromechanical conversion. In most cases the mechanical energy is required at variable speeds not at constant speeds and variable speed control for AC drives is not a trivial issue nowadays. The adjustable speed AC drives (ASD) is operated by supplying the electric motor drive with a variable amplitude and frequency three phase AC source. This variable frequency changes the motor speed because the rotor speed depends on the speed of the stator magnetic field which rotates at the same frequency of the applied voltage. A variable voltage is required because the current has to be limited by means of reducing the supply voltage as the motor impedance reduces at low frequencies.

At the time the above mentioned methodologies were being used for the speed control of AC motor drives, DC brush motors were already being used for adjustable speed drives with better speed and torque performance. The aim was to achieve an adjustable speed drive with good speed characteristics comparable to the brushed DC motor. Even after finding another AC asynchronous motor, also called induction motor, in 1883 by Tesla, more than six decades later of invention of DC brush motors, variable speed operation of ASD for induction motors is not as easy and effective as DC brush motors.

Speed control for DC motors is very easy to achieve. The speed is controlled by applied armature voltage and torque is controlled by armature current. In addition to it, DC brush motor drives are not only permitted four quadrant operations but also provide wide power ranges. Thus DC motors always have been the most preferred choice for use in high performance systems. The main and only reason for their popularity is the ability to control the torque and flux easily and independently. The separately excited DC motor where field excitation is provided externally has been used mainly for applications where there was a requirement for fast response and four-quadrant operation with high performance near zero speed.

The major disadvantage with DC motor is that it requires frequent maintenance and an eventual replacement of the brushes and commutators. It also precludes the usage of a DC motor in hazardous environments where sparking is not permitted. Also, there is a potential drop called associated with this arrangement, and is usually in the range of 1-1.5 V, leading to a drop in the effective input voltage. The DC brush motor, like any other rotating machine, has a stator and rotor (as shown in Fig. 1.1).

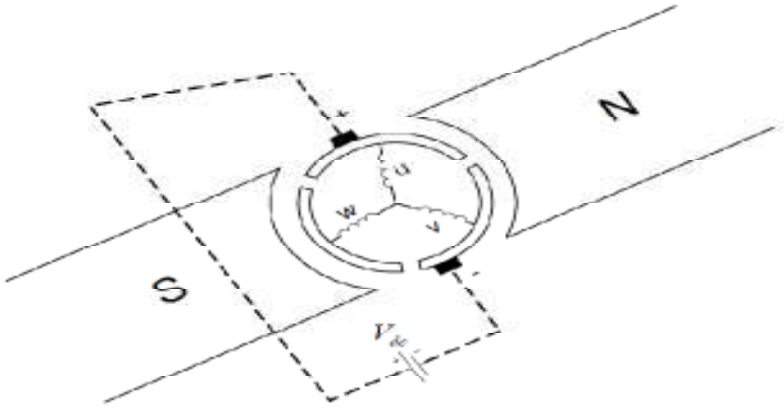

Fig.1.1 Basic model of a DC brush motor

On the stator (stationary part), there is a magnetic field system which can be provided either by permanent magnets or by excited field windings on the stator poles. On the rotor, the main components are the armature winding, armature core, a mechanical switch called commutator which rotates, and a rotor shaft. The commutator segments are insulated from one another. In addition to it, brushes, the stationary external components of the rotor, together with the commutator act not only as rotary contacts between the coils of the rotating armature and the stationary external circuit, but also as a switch to commutate the current flowing from the armature to the external DC circuit so that torque acting on it remains unidirectional even though the individual coil voltages are alternating. The maximum torque is produced when the magnetic field of the stator and the rotor are perpendicular to each other The commutator makes it possible for the rotor and stator magnetic fields to always be perpendicular. The commutation thus plays a very important part in the operation of the DC brush motor. It causes the current through the loop to reverse at the instant when unlike poles are facing each other. This causes a reversal in the polarity of the field, changing attractive magnetic force into a repulsive one causing the loop to continue to rotate.

As the back-EMF generated in the coil is short-circuited by the brush so, a large current flows causing sparking at the interface of the commutator and the brushes, as well as causing heating and the production of braking torque. In order to minimize this problem, commutation is carried out in the magnetic field crossover region. Even after taking these measures, because of the distortion of the effective magnetic flux due to the armature

reaction, some back-EMF is still generated in the coils in the magnetic field crossover region. It is desirable to minimize the crossover region in order to maximize the utilization of the motor. Thus though the AC motors are more rugged, cheap and less prone to failure but the controlling methods simplicity and performance is good for DC motors. These PM Brushless DC motors combine the features of both the AC and DC motor.

1.2 PERMANENT MAGNET MOTORS' DESCRIPTION

A brushless dc motor can be described as an inverted brush dc motor with its magnet being the rotor and its stationary windings forming the stator (In brushed DC motors, magnet forms the stationary part and windings, the rotating part). This design provides many advantages over the brush dc motor. Smooth and efficient operation of the brushless dc motor relies on knowledge of the energization sequence of the windings. Since there is no winding in the rotor (that would be supplied through the brushes), the AC PM machines are also called brushless PM machines. The rotor of the AC PM motor rotates synchronously with the magnetic field generated by the stator winding. Newly developed permanent magnet synchronous (PMS) motors with high energy permanent magnet materials particularly provide fast dynamics, very good compatibility with the applications and better power factor with efficient operation if they are controlled properly.

1.2.1 Classification of Permanent Magnet Motors

The permanent magnet (PM) synchronous machines can be widely classified based on the

a) Direction of field flux
b) Permanent magnets position
c) Rotor Position
d) Classification based on the shape of back-emf

1.2.1.1 Classification based on the direction of field flux

The Permanent magnet motors are of two types when classified on the basis of field flux direction. One is as *Radial field motors*, in which the flux direction is along the radius of the machine; and another as *axial field motors*, in which the flux direction is parallel to the rotor shaft. The radial-field PM machines are commonly used; however
the axial field machines are playing a significant role in a small number of applications because of their higher power density and acceleration.

1.2.1.2 Classification based on the position of Permanent Magnet

The Permanent Magnet motors are of two when classified on the basis of position of Permanent magnet in it. The magnets are mounted either on the surface of the rotor, called *surface mount permanent magnet motors (SMPM)* or are placed insides the rotor, called *interior permanent magnet motors (IPM).*

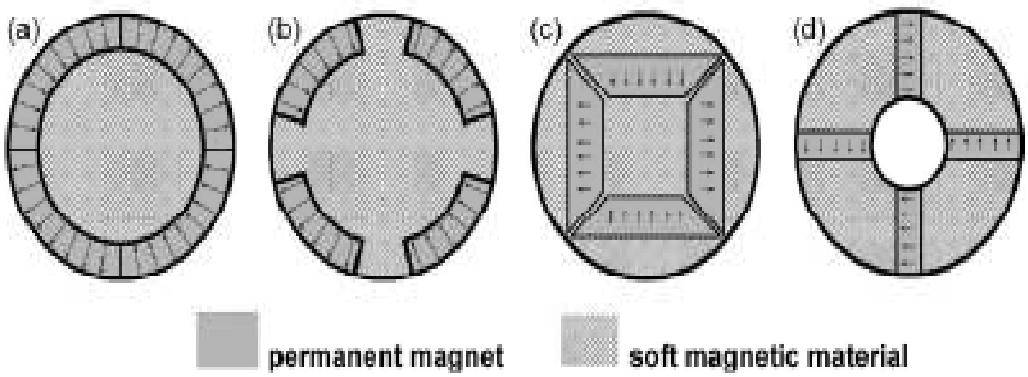

Fig 1.2 Classification of Permanent Magnet Motors based on the position of Permanent Magnet

IPM motors have superior characteristics compared to surface mount permanent magnet motors. This is because of some of their inherent characteristics like higher torque density and extended flux weakening region. These two advantages are because of their reluctance torque and ruggedness of the rotor structure. However, the Interior PM configuration produces considerable torque pulsation.

A SMPM motor cross-section view is shown in Fig.1.2 (a). It comprises of modern rare-earth materials with magnetic relative permeability close to unity, the effective air gap becomes equal to the sum of the physical air gap between rotor and stator in addition to the magnet depth. As a result of which, current flowing in armature conductors produces only a small magnetic-flux component, and therefore, the inductance of the phase winding is also small. Furthermore, if the entire rotor surface is covered by a permanent magnet, there is negligible variation in winding inductance with rotor position.

The inset magnet configuration is shown in Fig. 1.2(b). It is preferred for trapezoidal machines, because the magnet pole arc can be adjusted to assist in shaping the motional-EMF waveform. The presence of soft-magnetic material at the physical air gap in the

regions between the magnet poles causes a substantial variation in winding inductance, with maximum inductance occurring at rotor positions where the magnet pole arcs are misaligned from the winding axis.

Fig.1.2 (c) and (d) show have magnets buried in the rotor body. For the interior magnet structure shown in Fig. 1.2(c), the direction of magnetization is radial. This structure is preferred for sinusoidal PM machines, because it is easier to achieve the necessary sinusoidal variation of flux density around the air gap periphery. The high-permeability magnetic material adjacent to the air gap leads to higher values of machine inductances than those that occur in the first two configurations. Finally, the flux-concentrating type PM motor is shown in Fig. 1.2(d). It has magnets located with their axes in the circumferential direction, so that the flux over a rotor pole arc is contributed by two separate magnets. This configuration also exhibits significant saliency effects, causing a substantial variation of winding inductance with rotor position.

1.2.1.3 Classification based on the position of rotor

In this classification, permanent magnet motors are divided into *interior rotor* and *exterior rotor* structures.

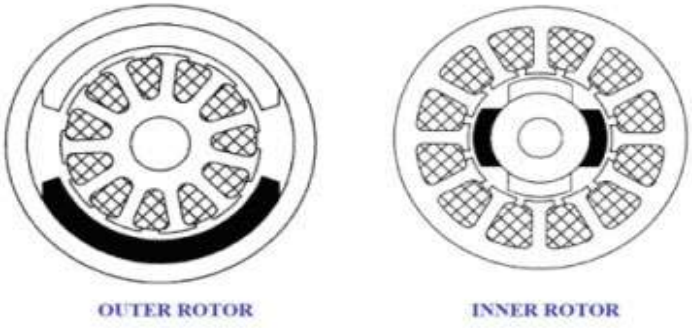

Fig. 1.3 Classification of Permanent Magnet Motors based on the position of Rotor

If rapid acceleration and deceleration of the load is needed in a specific application, as is the case for servo systems, then torque/inertia ratio of the motor should be as high as possible. Permanent magnet motors with interior rotor and high energy density magnets are good candidates for this application. Exterior rotor configuration is usually being used in application requiring constant speed such as fans and blowers. The spindle motor used in computers is of this category as well. The high inertia of the exterior rotor is an advantage in achieving uniform and constant speed.

1.2.1.4 Classification based on the shape of back-emf

Based on the shape of back-EMF waveform, permanent magnet motors are classified into permanent magnet brushless dc motors (BLDC) and permanent magnet synchronous motors (PMSM). The stator winding of a BLDC motor is wound such that the induced back-EMF is quasi-rectangular and that of PMSM is wound such that the induced back-EMF is sinusoidal. The sinusoidal type is known as permanent magnet synchronous motor; the trapezoidal type goes under the name of PM Brushless dc (BLDC) machine. Thus the PMSM has a sinusoidal back emf and requires sinusoidal stator currents to produce constant torque while the BDCM has a trapezoidal back emf and requires rectangular stator currents to produce constant torque. The PMSM is very similar to the wound rotor synchronous machine except that the PMSM that is used for servo applications tends not to have any damper windings and excitation is provided by a permanent magnet instead of a field winding.

1.2.1.5 Classification based on the saliency of rotor PM

These AC permanent magnet (PM) motors consists of a wound stator and a rotor. The stator may have a single-phase or multi-phase winding which is sometimes called the armature winding as in Fig. 1.1. The rotor just has permanent magnets. There are two types of rotors.

- Salient-pole rotor shown in Fig. 1.4 is mostly for low-speed machines.
- Cylindrical rotor shown in Fig. 1.5 is usually for high-speed machines.

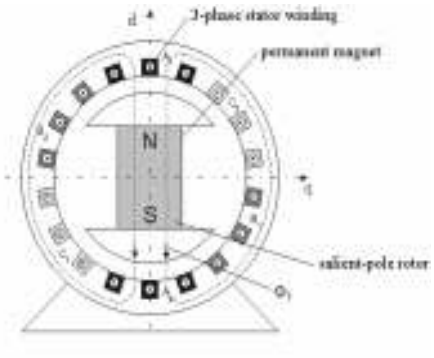

Fig. 1.4 Salient pole rotor

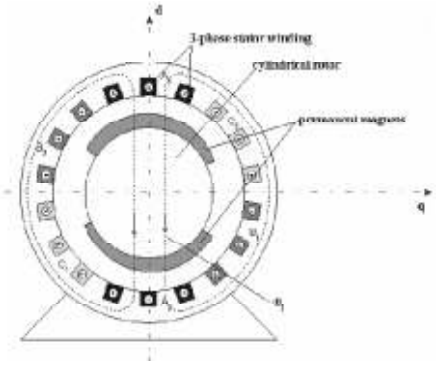

Fig. 1.5 Cylindrical pole rotor

1.2.2 Property of Permanent Magnet

The property of permanent magnet and the selection of pertinent materials are crucial in the design of permanent magnet machine. Barium and strontium ferrites are broadly used as permanent magnets. Low cost and huge supply of raw material are two major advantages of ferrite. They can be easily produced and their process is adopted for high volume as well as moderately high service temperature. The magnet has a practically linear demagnetization curve but has a low remnance. Therefore, the machine has a high volume as well as weight. The Cobalt-Samarium magnet is built of iron, Nickel, Cobalt, and rare-earth Samarium. High remnance, high energy density, and linear demagnetization characteristic are among its advantages. Although the material is quite expensive due to insufficient supply of Samarium, the service temperature can be as high as 300^{o} C and the temperature stability is very satisfactory. The Neodymium-iron-boron (Nd-Fe-B) magnet has the highest energy density, highest remnance, and very good coercivity. The disadvantages are low service temperature, and susceptibility to oxidation if it is not protected by coating. In addition, the temperature stability is lower than that of a CoSm magnet. Although the material is expensive compared to ferrite, the machine weight is reduced due to its higher energy density magnets. Nowadays, Nd-Fe-B magnets are being used in different applications.

1.2.3 Advantages over Brushed DC motors

The Permanent Magnet Brushless DC (BLDC) motor is the ideal choice for applications that require high power-to-volume ratio, high reliability, and high efficiency. BLDC motor is considered to be a high performance motor and is capable of providing large amounts of torque over a vast speed range. BLDC motors are a derivative of the most commonly used DC motor, the brushed DC motor, and they share the same torque and speed performance curve characteristics. The only major difference between the two is the use of brushes. BLDC motors do not have brushes so named "brushless DC" but the DC motors used to have brushes. Commutation is the process of changing the motor phase currents at the appropriate times of instants to produce rotational torque. In a brush DC motor, the motor assembly contains a mechanical commutator which is moved by means of actual brushes in order to move the rotor. A BLDC motor is highly reliable since it does not have any brushes to wear out and replace mechanical brushes. Instead of mechanical

commutation with brushes, electronic commutation is performed. This reduces friction, increases reliability, and decreases the cost to produce the motor itself. The tradeoff is more complex and expensive controllers. However, the economies of scale of electrical components are very different than those of the motors themselves, and a system-wide cost/performance evaluation favors brushless motors in many applications. So when operated, the life expectancy is over 10,000 hours. DC motors costs the time and money, perhaps a great deal depending on how long it takes to replace the worn part and get the process started again. Although a BLDC motor may cost more than a brushless motor, it will often more than pay for itself in the amount of work time saved.

1.2.4 BLDC Motor Advantages

Brushless dc motors are rapidly gaining popularity in the appliance, automotive, aerospace, consumer and industrial automation industries. Due to the absence of mechanical commutators and brushes and the permanent magnet rotor, brushless dc motors have several advantages over the brush dc and induction motor. Some of the advantages of brushless dc motors are:

(1) High power density, high torque to inertia ratio and high dynamic response due to the small size, low weight and high flux density neodymium-iron-boron permanent magnet rotor.

(2) Higher efficiency due to the low rotor losses as a result of the absence of current carrying conductors on the rotor and reduced friction and windage losses in the rotor.

(3) Long operating life and high reliability due to the absence of brushes and metallic commutators.

(4) Clean operation due to the absence of brushes, resulting in no brush dust during operation and allowing for clean room applications.

(5) Low audible noise operation due to the absence of brushes, commutators and smooth low air resistance rotor.

(6) High speed operation is possible, since these motors are electronically commutated and are not subjected to the limitations of conventional commutations.

(7) Low thermal resistance as most of the machine losses occur in the stationary stator, thereby allowing heat dissipation by the process of direct conduction. In addition, since the rotor losses are small, heat transfer to machine tools and work pieces when these

motors are utilized in machine tools is minimal, thereby reducing the effects of heat on the machining operation.

(8) Low Electromagnetic interference/RFI due to the absence of brushes and metallic commutators.

As a result of the above features, the brushless dc motor has been replacing other motors in many industries. The household appliance industry has been one of the fastest growing end product markets for adjustable speed drives. Brushless dc motors are now being used in refrigeration compressors, washing machines, fans, food processing equipment and vacuum cleaners in the household appliance industry. In the automotive industry, brushless dc motors are being used in fuel pumps, air-condition blowers and engine cooling fans. The exceptional features of brushless dc motors described above are responsible for their widespread use in many industries.

1.3 OBJECTIVE OF THE THESIS

The objective of the thesis is to evaluate the performance of PMBLDCM in various modes of operation. The commutation of the brushless DC motor can be carried out in several ways. The motor can be operated in open loop mode as well as closed loop mode. The industry's efficiency depends on the efficiency of the drive so the objective of the thesis is to do the analysis of its performance under various modes.

1.4 OUTLINE OF THE THESIS

This dissertation is divided into five chapters. **Chapter 1** gives the basic introduction about the PM motors and objective of the present work. **Chapter 2** presents a literature review of all the relevant research papers which are referred to in the process of pursuing this dissertation work. **Chapter 3** gives the description of the mathematical models of the supply and electrical and mechanical parts of the motor and MATLAB Simulation models for various controlling schemes. **Chapter 4** presents the simulation results obtained in the complete process. **Chapter 5** presents the conclusion of the thesis and also the future scope of work which can be carried out as an extension to this thesis.

1.5 CONCLUSION

Brushless dc motors are increasingly being employed in many high performance applications only because of the simplicity of their control. These have high power density, low inertia and high torque to inertia ratio and high dynamic response due to the small size, low weight and high flux density neodymium-iron-boron permanent magnet rotor. However, in many of these applications, constant ripple-free torque is an essential requirement. In an effort to broaden the range of applications for these motors, pulsating torque minimization techniques must be employed. The current drawn by the motor must have lower harmonics and controlling scheme should be so that ratings of the motor are not exceeded. Also the dependency of the PMBLDC motor on the sensor should get reduced as these affect the performance of the drive under sluggish, oily and dusty environment.

CHAPTER II

LITERATURE REVIEW

2.0 GENERAL

An extensive research work has been carried out in the field of permanent magnet drives since last few decades. These newly developed permanent magnet synchronous (PMS) motors with high energy permanent magnet materials provide fast dynamics, efficient operation and very good compatibility with the applications if they are controlled properly. As of the fact that the drives efficiency largely depends on the controlling methods, a large research work has been reported on its controlling algorithms. There are basically two types of Permanent magnet AC drives-PM synchronous motor drives and PM Brushless DC Motor drives. The PMSM is very similar to the wound rotor synchronous machine except that the PMSM that is used for servo applications tends not to have any damper windings and excitation is provided by a permanent magnet instead of a field winding. Hence the direct and quadrature axis (d, q) model of the PMSM can be derived from the well-known model of the synchronous machine. BLDC motors also have been gaining attention from various Industrial and household appliance manufacturers, because of its high efficiency, high power density and low maintenance cost. Due to recent developments in the fields of magnetic materials and power electronics and their applications to electric drives have increased significantly extent. The PMBLDC motor is found to be more efficient then the PMSM motor because of higher speed capability, larger application range from low speed to high speed and higher power density. Also PMBLDC motors have higher efficiency, higher power to weight ratio, higher torque to current ratio, faster dynamic response, less maintenance, better power factor and better output power per unit mass and volume as compared to the conventional motors.

2.1 LITERATURE SURVEY

The existing literature survey available on Permanent Magnet Motors are classified into two categories:

2.1.1 Literature Review on PMSM

Pragasan Pillay et al. [1] studied the two types of permanent-magnet ac motor drives available in the drives industry. These are the PM synchronous-motor (PMSM) drive with a sinusoidal flux distribution, and the PM BLDC motor drive with a trapezoidal flux distribution. The application of vector control to the PMSM and complete modeling, simulation, and analysis of the drive system is described. The state-space models, speed controller and the inverter switches and vector controller are also included in the study. Performance differences due to the use of pulse width-modulation (PWM) technique and hysteresis current controllers are also examined. But the main attention is paid to the motor torque pulsations and speed response.

R. Krishnan [2] reviews the operation of the PMSM Drives when it is constrained to be within the permissible envelope of maximum inverter voltage and current to produce the rated power. Due to the constraints on the available dc link voltage and current rating of an inverter, the motor input voltage and current ratings also get limited. This limited voltage and current impact the maximum speed up to which constant rated torque is available and the maximum torque producing capability of the motor drive system, respectively. It is required and desirable to produce the rated power with the highest attainable speed for many applications such as electric vehicles, golf carts, forklifts, machine tool spindle drives etc. The rated power is for steady state operation and multiple times that is preferred for flat accelerations and decelerations during transient operation. From these considerations, this paper addresses the steady state operation, transient operation, and control techniques for the PMSM drives in the field weakening region.

Pragasan Pillay et al. [3] present the dynamic models and equivalent circuits of two PM machines. It has shown that although the PMSM and the BDCM are similar in construction, their modeling takes different forms. The d, q model of the wound rotor SM is easily adapted to the PMSM while an abc phase variable model is necessary for the BDCM if a detailed study of its behavior is needed. Because of the non-sinusoidal variation of the mutual inductances between the stator and rotor in the BDCM, it is also shown in this paper

that no particular advantage exists in transforming the abc equations of the BCDM to the d, q frame. Hence the solution of the original abc equations is proposed for the BDCM.

Javad Soleimani et al. [4] presents the mathematical model of 3-phase PMSM based on dq axial model presents and for different permanent magnets having same volume and thickness, extracted necessary parameters for this modeling. Effect of various permanent magnets on power factor and torque is investigated for a traction load. It is deduced from results that using more suitable hard magnetic materials increase power factor. Torque response and power factor for each material investigated and it has been investigated that the increment of mechanical torque applied to motor, using permanent magnet with low B and H, in the motor prevents to reaching synchronous state. In other word, motor is not compatible with this load. While permanent magnet's volume is suitable, using hard magnetic material with high B and H have remarkable effect on time of synchronization or settling time and torque ripple.

Salih Baris Ozturk et al. [5] presents a direct torque control (DTC) scheme for PM synchronous motors (surface-mount type) using hall-effect sensors in constant torque region. This scheme requires no dc-link sensing and removes some common problems those conventional DTC drives suffer from such as the effect of resistance change, low speed operation integration drift, and the initial rotor position requirement.

Badre Bossoufi et al. [6] presents a modeling of unit PMSM, inverter of tension and order known as DTC under Matlab/Simulink. The DTC scheme allows independent control for the torque and flux, an optimal response time; it does not have the mechanical sensors and allows obtaining excellent dynamic performances.

G. Foo et al. [7] presents a novel stator flux observer for DTFC of IPMSM drives. The observer is based on the extended rotor-flux concept, which transforms an IPMSM into a Surface mounted PM one. Direct torque and flux control (DTFC) of IPMSM is known to deliver fast torque and flux dynamic responses. But its flux estimation at very low speeds has been the largest drawback. A multitude of flux observers have been proposed for flux estimation but most of them fail to give fair performance in the low-speed region. This scheme proposes a new stator flux observer for improved flux estimation at very low speeds. This observer is based on the extended rotor flux concept which is combined with

the DTFC scheme to achieve a high performance sensorless IPMSM drive over a wide speed range, including standstill.

Gilbert Foo et al. [8] investigates a modified direct torque control (DTC) scheme based on space vector modulation (SVM) for Interior PM Synchronous motor (IPMSM) drives. Closed-loop control of both the flux linkage and torque are achieved. The modified DTC utilizes two PI controllers to regulate the torque and stator flux linkage independently. The reference voltage vector is synthesized with the SVM technique as opposed to the switching table in the classical DTC. As a result, the torque and flux ripples are significantly lower in the new scheme while retaining its main advantages.

Lang Baohua et al. [9] presents a space vector modulation method which is applied to direct torque control system structure. The scheme maintains the characteristics of the traditional direct torque control but simultaneously improves the torque ripple effectively and makes the inverter switching frequency constant. The fundamental difference between these two methods is that the traditional DTC has only six effective voltage vector and uses hysteresis controllers, while the SVM-DTC can use any linear combination of required voltage vector and so can more accurately control the stator flux movement.

Bhim Singh et al. [10] deals with the DSP based implementation of a Sliding Mode (SM) speed controller for DTC of Permanent Magnet Synchronous Motor (PMSM) drive. The drive system consists of power circuit and control hardware. The former has IGBT based voltage source inverter (VSI) and gate driver circuit, while the latter has voltage and current sensors and the interfacing circuits. The assembly language programming used for the implementation on DSP has resulted in giving faster and good response. Moreover, any modification in control structure is easily possible by changing the software to meet the requirements of a specific application. The rotor speed estimation from the sensed position signals, SM speed controller, torque, flux, and sector estimator and optimum voltage vector selection table for gating pulse generation of VSI are implemented in assembly language of DSP-ADMC401.

M. B. B. Sharifian et al. [11] deals with the two popular and powerful methods- field oriented control (FOC) and space vector modulation (SVM). The FOC-SVM method has been incorporated with a predictive current control (PCC) technique. This method estimates the desirable electrical torque to track mechanical torque at a reference speed of PMSM.

The estimated torque is then used to calculate the reference current based on FOC. In order to increase the performance of the traditional SVM a predictive current control (PCC) method is established as a switching pattern modifier. The performance of the controller is then evaluated in terms of torque and current ripple and the transient response to step variations of the torque command.

2.1.2 Literature Review on BLDC Motor

Ji Hua, Zibo et.al [12] presents the mathematical model of the BLDCM, the modeling and simulation of the control system of brushless DC motors (BLDCM). By the organic combination of these blocks, the simulation model of control system for BLDCM has been established. The control system can operate stably and has the fairly good dynamic and static characteristics. Using this simulation model built for BLDCM, control algorithms can be verified conveniently. Through the modularization design, a lot of time of engineers design can be saved and the design efficiency can be promoted rapidly.

Vinatha U et al. [13] presents a modeling procedure that helps in simulation of various operating conditions of BLDC drive system. The performance evaluation results show that, such a modeling is very useful in studying the drive system before taking up the dedicated controller design, accounting the relevant dynamic parameters of the motor.

Pragasan Pillay et al. [14] presents the modeling, simulation, and analysis of a BDCM drive. Particular attention is paid to the motor large- and small-signal dynamics and motor torque pulsations. The simulation included the state space model of the motor and speed controller and real-time model of the inverter switches. Every instance of a power device turning on or off is simulated to calculate the current oscillations and resulting torque pulsations. The results indicate that the small and large signal responses are very similar. This result is only true when the timing of the input phase currents with the back EMF is correct. The brushless dc motor has a permanent-magnet rotor, and the stator windings are wound such that the back electromotive force (EMF) is trapezoidal. It therefore requires rectangular-shaped stator phase currents to produce constant torque. The trapezoidal back EMF implies that the mutual inductance between the stator and rotor is non-sinusoidal. Therefore, no particular advantage exists in transforming the machine equations into the

well-known two-axis equations, which is done in the case of machines with sinusoidal back EMF's i.e. PMSMs.

Nicola Bianchi et al. [15] presents an overall comparison between motor configurations and high-frequency voltage injection techniques. It investigates the response to a high-frequency voltage injection of two rotor configurations: an IPM rotor with three flux-barriers per pole and an inset rotor, with iron teeth separating the adjacent surface-mounted PMs. Both high-frequency pulsating and rotating voltage injection techniques are used to detect the rotor position angle. The effectiveness of the rotor position detection is investigated under several operating conditions, which means for various torque requirements.

Yoseph Buchnik et al. [16] proposes a method to detect and control the speed and the position of a BLDC motor with a low resolution position encoder in very low speeds of several rad/sec. The low resolution encoder could be the Hall Effect sensor that has a resolution of maximum 60 electrical degrees, according to the pole number of the motor. The algorithm uses a Kalman Filter (KF). The position and the current are sampled. It would be possible to detect low rotation speeds with a low-resolution position encoder by using a KF, while the position and the current are measured.

Balogh Tibor et al. [17] presents a model of brushless DC motor considering behavior of the motor during commutation. The torque characteristic of BLDC motor presents a very important factor in design of the BLDC motor drive system, so it is necessary to predict the precise value of torque, which is determined by the waveforms of back-EMF. After development of simple mathematical model of the BLDC motor with sinusoidal and trapezoidal waveforms of back-EMF the motor is simulated in the MATLAB/Simulink environment. The performance evaluation results show that, such a modeling is very useful in studying the drive system before taking up the dedicated controller design, accounting the relevant dynamic parameters of the motor.

R. Somanatham et al. [18] presents a scheme for the modeling and simulation of sensorless control of Permanent Magnet Brushless DC (PMBLDC) motor using zero-crossing back e.m.f technique. Since the neutral point of star connected machine is floating and not accessible to detect zero-crossing points, line back e.m.f information is considered. The motor is commutated at zero-crossing point of back e.m.f. When the motor reaches the

minimum speed to facilitate zero-crossing detection of back e.m.f, the control is transferred to zero crossing detection circuit. The main advantage of the scheme is that the sensorless operation can be easily implemented without the neutral point.

Boyang–Hu et al. [19] describes a novel sensorless-drive method of 180-degree commutation of BLDCM. Inverter gate signals are generated by comparing the polarities of the estimated back-emf signals. The estimated trapezoidal back-emf signals are obtained by sensing the three phase-current of motor and the inverter output voltage. Rather than the conventional estimation methods, the proposed method cancels the complicated calculation-steps, which can burden DSP in practical experiments.

Y. S. Jeon et al. [20] illustrates a method for the reduction of error in simulation, for that purposes a new simulation model of BLDC motor with nearly real back EMF waveform. The torque characteristic of BLDC motor is very important factor in the design of motor drive system, so it is necessary to predict the precise value of torque, which is determined by the waveform of back EMF. This scheme considers the fact that due to the shapes of slot, skew and magnet of BLDC motor, the real back EMF waveform is at some degree deviated from the ideal trapezoidal waveform. As a result, when using the ideal trapezoidal waveform, the error occurs. In consequence, in order to lessen such an error, the model of BLDC motor with real back EMF waveform is needed instead of its approximation model. So for the reduction of error in simulation, a new simulation model of BLDC motor with nearly real back EMF waveform is proposed which is restored by FFT and IFFT method to improve simulation result of BLDC motor.

Somesh Vinayak Tewari et al. [21] proposes a method of minimization of torque ripple of brushless dc (BLDC) motors, with un-ideal back EMF under MATLAB 7.1/Simulink environment. An idealized BLDC motor has trapezoidal back EMF waveform. However, for practical reasons like non-uniformity of magnetic material and design trade-off it is hard to produce desired trapezoidal wave shape. Therefore torque ripple appears in conventional control. In this scheme, the duty cycle of the pulses is calculated in the torque controller in both normal conduction period and commutation period and in combination with a given commutation sequence fed to the inverter gates so as to minimize ripple. Moreover, the influence of finite dc supply voltage is considered in commutation period. Simulation results show that compared with conventional control, this method results in apparent

reduction of torque ripple. This reduced torque pulsations makes it extremely suitable in applications such as position sensing and robotics. The reduced ripples in torque also help in eliminating undesirable noise and inaccuracies in motion control.

K. S. Rama Rao et al. [22] proposes a scheme for sensorless control of a brushless dc (BLDC) motor by direct back EMF detection method using dsPIC30F3010. A mathematical model of the drive system is simulated with MATLAB SIMULINK Toolbox. As the terminal voltage of the motor is proportional to the phase back EMF on the floating phase, the DSP-ADC feature utilized to sense the back EMF proves the validity of sensorless control over a wide speed range. The experimental results obtained using the proposed BLDC drive system have proved the simplicity of the application of dsPIC30F3010 microcontroller for sensorless speed control.

Jianwen Shao [23] demonstrates that the direct back-electromotive-force (EMF) detection method previously described in a sensorless brushless dc (BLDC) (Proc. IEEE APEC, 2002, pp. 33–38) motor-drive system synchronously samples the motor back EMF during the pulse width modulation (PWM) off time without the need to sense or reconstruct the motor neutral. Since this direct back-EMF-sensing scheme requires a minimum PWM off time to sample the back-EMF signal, the duty cycle is limited to something less than 100%. So an improved direct back-EMF detection scheme that samples the motor back EMF synchronously during either the PWM on time or the PWM off time is proposed to overcome the problem.

Wook-Jin Lee et al. [24] presents a novel method to detect the rotor position of the Brushless DC (BLDC) motor at standstill and a start-up method to accelerate the rotor up to a certain speed where the conventional position sensorless control methods based on the back EMF could work reasonably. The principle of the estimation is based on the variation of the current response caused by the magnetic saturation of the stator core of BLDC motor when the current flows along the magnetic axis. The method can be implemented using only one current sensor at DC link of the inverter. It does not depend on the model of the motor, and it is robust to motor parameter variations. By the method it has been demonstrated that the motor can restart smoothly without failure even after severe disturbance during the starting procedure.

Yen-Shin Lai et al. [25] presents a field programmable gate array-based BLDCM driver system set up to calculate the zero-crossing point of back EMF at both low and high speed regions. For the present technique, the experimental results show the duty can be smoothly controlled from 5% to 95% while not invoking any position and current sensors. The zero crossing point of back-EMF which is used for generating proper commutation control of inverter is calculated by sampling the voltage of floating phase. Therefore, no current and position sensors are required for the implementation. The method can be easily implemented using digital controller.

J. X. Shen et al.[26] demonstrates the application of third harmonic back-EMF-based sensorless rotor position estimation to both BLDC machines. The sensorless control of brushless machines by detecting the third harmonic back electromotive force is a relatively simple and potentially low-cost technique. It caters for phase currents which flow continuously, when the zero crossings of the phase back-EMF waveforms are not detectable. However, as with all EMF-based sensorless methods, an open-loop starting procedure still has to be employed.

J. X. Shen et al. [27]develops an improved ASIC based controller using the third harmonic back EMF instead of the terminal voltages. Application-specific integrated circuit (ASIC) ML4425 is often used for sensorless control of permanent-magnet (PM) brushless direct current (BLDC) motor drives. It integrates the terminal voltage of the un-energized winding that contains the back electromotive force (EMF) information and uses a phase-locked loop (PLL) to determine the proper commutation sequence for the BLDC motor. However, even without pulse-width modulation, the terminal voltage is distorted by voltage pulses due to the free-wheel diode conduction. The pulses, which appear very wide in an ultrahigh-speed (120 kr/min) drive, are also integrated by the ASIC. Consequently, the motor commutation is significantly retarded, and the drive performance is deteriorated. But the ASIC integrate the third harmonic back EMF instead of the terminal voltage, such that the commutation retarding is largely reduced and the motor performance is improved. It also uses the integration of third harmonic back EMF and the PLL technique and provides controllable advanced commutation to the BLDC motor.

Maher Faeq et al. [28] presents an improved sensorless controller using third harmonic back-EMF with software phase locked loop has been develops to get precise commutation

sequence. This method show a good improvement in commutation pulse at high speed thus the phase current is minimally delayed from the back-EMF, and hence leading to improved power factor and higher torque production than those obtained using a conventional back-EMF zero crossing method. In general, the average torque falls rapidly as the rotor speed increases above the base speed, hence the motor will frequently be found to have insufficient torque at higher speed. One way to counter this problem is by using third harmonic back-emf detection technique during high speed operation because the third harmonic is usually kept a constant relationship with rotor position for any motor speeds and load conditions. Furthermore this method is practically free of noise which may be introduced from inverter switches.

Kuang-Yao Cheng et al. [29]presents the design and realization of a sensorless commutation integrated circuit (IC) for brushless dc motors (BLDCMs) by using mixed-mode IC design methodology. This IC can generate accurate commutation signals for BLDCMs by using a modified back-EMF sensing scheme instead of using Hall-effect sensors. This IC can also be easily interfaced with a microcontroller or a digital signal processor (DSP) to complete the closed-loop control of a BLDCM. The sensorless commutation IC consists of an analog back-EMF processing circuit and a programmable digital commutation control circuit. Since the commutation control is very critical for BLDCM control, this sensorless commutation IC provides a phase compensation circuit to compensate phase error due to low-pass filtering, noise, and non-ideal effects of back-EMFs. By using mixed-mode IC design methodology, this IC solution requires less analog compensation circuits compared to other commercially available motor control ICs. Therefore, high maintainability and flexibility can be both achieved.

A. Ungurean et al. [30]introduces a novel sensorless control of brushless dc permanent magnet (BLDC-PM) motor based on I-f principle for starting (from any initial position) with seamless commutation to BEMF zero crossing detection above a certain speed. The starting method assures a fast response and the criteria for switching to speed sensorless control introduces short transients. This way, for general drives, even with notable load torque at start, the motor will start, although after a short hesitation depending on the initial position of the rotor. Also, the condition to switch between I-f control and sensorless

control assures short transients. It had been proved that I-f starting strategy (simulation results) can assure faster response than V/f starting.

Alin Ştirban et al. [31] introduced a FEM assisted position and speed observer for brushless dc PM motor drive sensorless control, based on the line-to-line PM flux linkage. The line-to-line PM flux linkage can be estimated from measured phase currents and measured line-to- line voltages. The zero-crossing of the line-to-line PM flux occurs right in the middle of two commutations points. This is used as a basis for the position and speed observer. This sensorless control method is used together with the If sensorless control, for start-up and for low speed control, with seamless transitions between them. Digital simulations and experimental results demonstrate that the FEM assisted position and speed observer for BLDC PM motor sensorless control operation, provides rather precise commutation points, even during speed or load transient states.

Yuanyuan Wu et al. **[32]** presents a novel arithmetic for sensorless BLDC motor drives. Based on the characteristics of the back electromotive force (EMF), the rotor position signals would be constructed. It is intended to construct these signals, which make the phase difference between the constructed signals and the back EMFs controllable. Then, the rotor-position error can be compensated by controlling the phase-difference angle in real time. The rotor-position-detection error is analyzed using the TMS320F2812 chip as a control core.

Paul P. Acarnley et al. [33] reviews the state of the art in these sensorless techniques, which are broadly classified into three types: motional electromotive force, inductance, and flux linkage.

P. Damodharan et al. [34] describes a position sensorless operation of permanent magnet brushless direct current (BLDC) motor. The position sensorless BLDC drive proposed is based on detection of back electromotive force (back EMF) zero crossing from the terminal voltages. This difference of line voltages provides an amplified version of an appropriate back EMF at its zero crossings. The commutation signals are obtained without the motor neutral voltage. Only three motor terminal voltages need to be measured thus eliminating the need for motor neutral voltage. While starting relies on triggering devices at the zero crossings detected using the above algorithm, continuous running is achieved by realizing the correct commutation instants 30◦ delay from the zero crossings.

Carlo Concari Fabrizio Troni [35] describes a control technique suitable for low speed sensorless operation of BLDC motors based on BEMF reconstruction The proposed control technique does not require heavy hardware modification to basic BLDC sensorless control schemes; only phase motor voltage measurement is necessary. Extensive simulations are performed in order to assess the validity of the proposed technique in operating conditions similar to those encountered in the DSP implementation. Experimental results confirm that the control has good dynamic performance and good regulation of the speed loop; moreover, it is rather insensitive of voltage measurement offsets and current ripple, so that reliable sensorless operation is ensured also at low speed.

Satoshi Ogasawara et al. [36] presents a position-sensorless brushless dc motor in which the position information is given on the basis of the conducting state of free-wheeling diodes in an open phase. The open phase current under chopper operation results from the back emf's produced in the motor windings. Therefore, this is considered to be an indirect detection of the back emf's through the free-wheeling diodes. This approach is characterized by its sophisticated position detection and makes it possible to detect the rotor position over a wide speed range from 45 to 2300 r/min compared with the conventional method that directly detects the back emf's. This sensorless position-detecting method, however, requires the inverter to be operating in a chopping mode in order for the algorithm to work properly.

E. Kaliappan et al. [37] describes a simple and improved sensorless technique for position and speed control of PMBLDC motor .In the technique, instead of using the zero crossing time, the Back EMF voltage at the middle of commutation period is used as a control variable. In the proposed sensorless technique, without using the motor neutral voltage, the Back EMF of the floating phase which is detected during the PWM off time is used. This simplified and improved sensorless technique does not require any filtering.

Fernando Briz et al. [38] analyzes saliency-based sensorless control methods for ac machines. This focuses on three different saliency-based sensorless methods for ac machines: negative-sequence carrier-signal-current-based methods, zero-sequence carrier-signal-voltage-based methods, and zero-sequence PWM-switching-voltage-based methods. Applicability of these methods for both rotor position estimation (tracking of rotor-

position-dependent saliencies) and flux position estimation (tracking of flux-dependent saliencies) is studied for each method, as well as aspects of their implementation.

Ajay Kumar Bansal et al. [39] purposes an algorithm using fuzzy logic to estimate the speed and position of BLDC motor from back EMF for sensorless brushless DC (BLDC) motor drives to improve the performance of conventional sensorless drives. Conventional sensorless methods of the BLDC motor drive have low performance under transient state or low speed range or under speed reversal. They occasionally require additional circuit. To cope with this problem, a fuzzy back-EMF estimator using the commutation function estimates the back-EMF of trapezoidal shape. As a result, this sensorless drive method without additional circuit has higher performance than conventional sensorless methods.

A. Albert Rajan et al. [40] purposes a new reconfigurable digital controller for BLDC motor. This paper focuses on reconfigurable controller using fuzzy logic technique for a BLDC motor for variable frequency and variable duty ratio operation. In digital controller of brushless DC motor, the control accuracy is of a high level, and it has a low response time; furthermore, this technique is implemented using reconfigurable Vertex II Pro development board. This propose energy efficient controller consumes 70 mW, which is less compared to other conventional controllers.

Atef Saleh Othman Al-Mashakbeh [41] describes a mathematical model of brushless DC motor and the PID control based on the Ziegler-Nichols method is presents using the software package MATLAB/SIMULINK. The simulated system has a fast response with small overshoot and zero steady state error. The PID controller designed has been simulated and observed to have good performance.

Tribeni Prasad Banerjee et al. [42] purposes a hybrid motion control technique, which is develops and implemented in real time. The technique is tested online on the motor using the TMS 320F 2812 board. The offline and online test results show that the proposed technique is able to discriminate between fault and normal (unfaulted) currents with high accuracy. This technique does not require any harmonic contents analysis. The proposed technique is quite fast and easy to implement. It requires less computational memory for the online implementation.

G. H. Jang et al. [43] presents a method of identifying the rotor position of a BLDC motor and of driving a motor from standstill smoothly without any position sensors, using the

inductance variation of the rotor position. This is done by monitoring the current responses to the inductance variation on the rotor position. A controller for a BLDC motor is developed using a PC, digital signal processor (DSP), and inverter and communication circuits in order to verify the proposed algorithm experimentally.

2.2 CONCLUSION

There is large scope of research work in Permanent Magnet Motor Drives. Better operating performances have been achieved with sensors and without sensor. A lot many controllers have been used in order to test the performance characteristics of the PM motors, which have also resulted in improved performance. Simplicity of controlling technique also matters a lot. It should also be kept in mind that the cost factor is not too high for the low power rating machines. So depending upon the application area, its cost, simplicity and suitable controlling technique must be used.

CHAPTER III

MATHEMATICAL MODELING OF PMBLDC MOTOR AND MATLAB SIMULATION

3.0 GENERAL

Mathematical modeling is the art of translating problems from an application area into tractable mathematical formulations whose theoretical and numerical analysis provides insight, answers, and guidance for designing improved behavior before a prototype system is actually manufactured. A mathematical model is an analytical description of a system using mathematical concepts and language. The process of developing a mathematical model is termed mathematical modeling. Mathematical models are used not only in the natural sciences (such as physics, biology, earth science, meteorology) and engineering disciplines (e.g. computer science, artificial intelligence), but also in the social sciences (such as economics, psychology, sociology and politicalscience); physicists, engineers, statisticians, operations research analysts and economists use mathematical models most extensively. A model may help to explain a system and to study the effects of different components, and to make predictions about behavior. Mathematical models can take many forms, including but not limited to dynamical systems, statistical models, differential equations, or game theoretic models. In many cases, the quality of a scientific field depends on how well the mathematical models developed on the theoretical side agree with results of repeatable experiments.

3.1 MODELING OF SUPPLY TO PMBLDC

The supply that is fed to the stator of Permanent magnet BLDC motor is preferred to be variable voltage variable frequency so as to control it. So before the AC supply is fed to stator, it passes through following blocks

3.1.1 AC to DC Diode Bridge Rectifier

Power circuit of BLDCM drive is comprised of a for a three phase bridge rectifier using six diodes is shown in fig 3.1. The diodes are arranged in the three legs. Each leg has two series connected diodes. Upper diodes constitute the positive group of diodes and lower diodes constitute the negative group of diodes. This rectifier is called 3-phase 6-pulse diode rectifier, 3-phase full wave rectifier or three phase B-6 diode rectifier.

The average value of output voltage is given by

$$V_o = \frac{3*\sqrt{6}}{pi} V_p \qquad (3.1)$$

Where V_p is the rms value of phase voltage and V_o is the average output voltage.

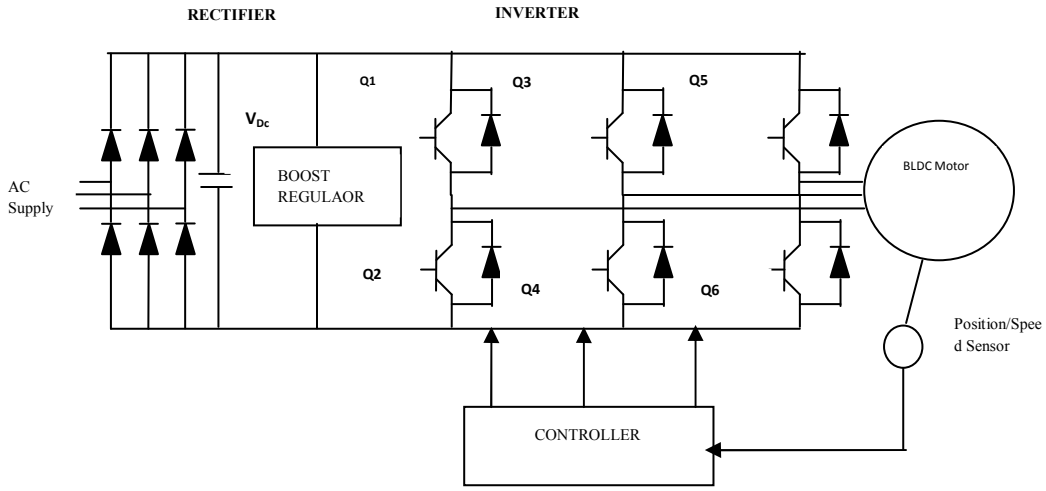

Fig 3.1 Supply system to PBLDC motor

The average value obtained is fixed but it is not necessary always that this fixed voltage is desirable so need a boost Regulator which can boost the level of this DC (average output) voltage as per the requirement

3.1.2 Boost Regulator

In this boost Regulator, the output voltage is greater than the input voltage- hence the name "boost". The output voltage of the three phase diode bridge rectifier is given as an input to the boost regulator which boosts the input voltage depending upon the "turn on" period of the switch (Mosfet switch shown here). The circuit arrangement of a boost regulator is shown in fig 3.2

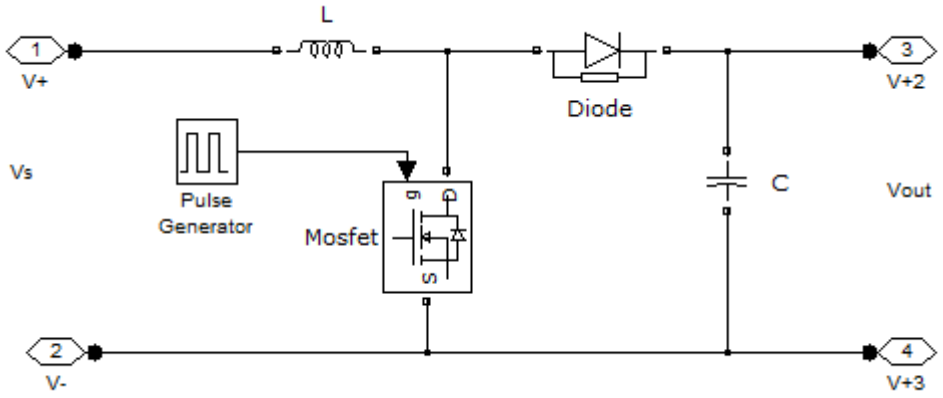

Fig 3.2 Boost regulator circuit diagram

The output voltage of the boost regulator is given by the expression

$$V_{out} = \frac{1}{(1-k)} * V_s \tag{3.2}$$

where k is the turn on time of switch e.g. if k=0.5 then output voltage is twice that of input voltage.

Parameters used in boost regulator block in the present work are listed in table 3.1

Table 3.1 Boost Regulator Specification

L	150e-6 H
C	2220e-6 F
Time period of pulse given to switch	40e-6 seconds
Pulse width, T_{on} (% of period)	80%
Resistance (On)	0.001 ohms

3.1.3 Inverter Unit

A device that converts DC power into AC power at desired output voltage and frequency is called an inverter. Industrial applications of inverters are mainly for adjustable-speed ac drives, induction heating, UPS for computers etc.

3.1.3.1 Three phase Bridge Inverter

For providing adjustable-frequency power to PMBLDCM, three phase inverters are more commonly used. Three phase inverters, take their dc supply from a battery or more usually from a rectifier. Here the dc voltage output of the boost-regulator is fed as an input to the inverter unit which converts it into three phase variable voltage variable frequency supply which is then fed to the stator of PMBLDC motor.

A basic three phase inverter is a six-step bridge inverter. Inverter unit is shown on right half of fig 3.1. It uses a minimum of six IGBTs. In inverter terminology, a step is defined as a change in the firing sequence from one IGBT to another in proper sequence. For one cycle of 360^o, each step would be of 60^o interval for a six step inverter. This means that IGBT would be gated at regular interval of 60^o in a proper sequence so that a 3 phase ac voltage is synthesized at the output terminals of a six-step inverter. Table 3.2 lists the parameters of the inverter.

Table 3.2 Inverter Specification

Power Electronic device used	IGBT/Diodes
Number of arms	3
Snubber Resistance	5000 ohms
Snubber Capacitance	1e-6 F

3.2 MATHEMATICAL MODELING OF PERMANENT MAGNET BLDC MOTOR

3.2.1 Three Phase Stator Equations

The coupled circuit diagram of three phase stator is shown in fig. 3.3. The equations of the stator windings in terms of motor electrical constants are

$$V_{an} = R_a i_a + \frac{d}{dt}(L_{aa} i_a + L_{ba} i_b + L_{ca} i_c) + e_a \quad (3.3)$$

$$V_{bn} = R_b i_b + \frac{d}{dt}(L_{ab} i_a + L_{bb} i_b + L_{cb} i_c) + e_b \quad (3.4)$$

$$V_{cn} = R_c i_c + \frac{d}{dt}(L_{ac} i_a + L_{bc} i_b + L_{cc} i_c) + e_c \quad (3.5)$$

where $R_a, R_b, R_c = R$ Stator resistance per phase, assumed to be equal for all phases.

$L_{aa}, L_{bb}, L_{cc} = L_s$ Stator inductance per phase, assumed to be equal for all phases.

$L_{ba}, L_{ab}, L_{ac}, L_{ca}, L_{bc}, L_{cb} = M$ Mutual inductance between the phases, assumed to be equal for all phases.

i_a, i_b, i_c	Stator current/phase.
V_{an}, V_{bn}, V_{cn}	Stator voltages/phase
e_a, e_b, e_c	Induced emf/phase

As the stator is star connected so taking $i_a + i_b + i_c = 0$ we get the equations (3.3) to (3.5) as

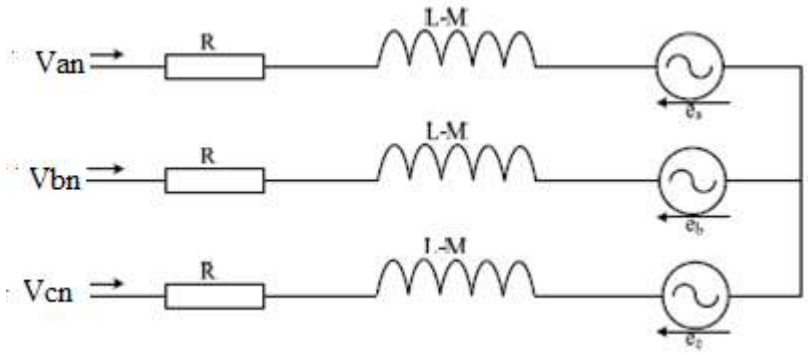

Fig 3.3 Three phase stator voltage circuit representation of PMBLDC motor

$$V_{an} = R i_a + (L_s - M)\frac{d}{dt} i_a + e_a \quad (3.6)$$

$$V_{bn} = R i_b + (L_s - M)\frac{d}{dt} i_b + e_b \quad (3.7)$$

$$V_{cn} = Ri_c + (L_s - M)\frac{d}{dt}i_c + e_c \quad (3.8)$$

The instantaneous induced emf is given by

$$e_a = f_a(\theta_r)\lambda_p\omega_m \quad (3.9)$$

$$e_b = f_b(\theta_r)\lambda_p\omega_m \quad (3.10)$$

$$e_c = f_c(\theta_r)\lambda_p\omega_m \quad (3.11)$$

where ω_m is the mechanical speed of the rotor (rad/sec), θ_r is the electrical rotor position (rad) and λ_p is the linking flux.

The electromagnetic torque produced by the BLDC motor is given as

$$T_e = \lambda_p[f_a(\theta_r)i_a + f_b(\theta_r)i_b + f_c(\theta_r)i_c] \quad (3.12)$$

3.2.2 Mechanical Equation

The mechanical equation of motion for simple system is,

$$T_e = J\frac{d\omega_m}{dt} + T_l + \mathrm{B}\omega_m \quad (3.13)$$

Where T_e, the electromechanical torque is produced by the motor, T_l is the load torque, J is the inertia and B is the frictional constant.

Speed can be calculated from equation 3.13 as

$$\frac{d\omega_m}{dt} = \frac{1}{J}(T_e - T_l - \mathrm{B}\omega_m) \quad (3.14)$$

Once the angular speed is calculated the rotors' mechanical position as well as electrical position can be estimated. The relation between angular velocity and angular position is given by

$$N = \frac{30}{pi} * \omega_m \quad (3.15)$$

Where N is the speed in rpm.

$$\frac{d(\theta_r)}{dt} = \frac{P}{2}(\omega_m) \quad (3.16)$$

Where P, the total is number of poles and θ_r is the electrical angular position.

3.2.3 Relation between Electrical and Mechanical equation

The back-emf ($e_a, e_b \; and \; e_c$) of the Permanent magnet BLDCM is a function of state variable (θ_r), rotor electrical position, which is given as the trapezoidal function and is written as a function

$$\begin{aligned} f_a(\theta_r) &= 1 && 0 < \theta_r < \frac{\pi}{3} \\ &= \left(\frac{\pi}{2} - \theta_r\right) * \frac{6}{\pi} && \frac{\pi}{3} < \theta_r < \frac{2\pi}{3} \\ &= -1 && \frac{2\pi}{3} < \theta_r < \pi \\ &= -1 && \pi < \theta_r < \frac{4\pi}{3} \\ &= \left(\theta_r - \frac{3\pi}{2}\right) * \frac{6}{\pi} && \frac{4\pi}{3} < \theta_r < \frac{5\pi}{3} \\ &= 1 && \frac{5\pi}{3} < \theta_r < 2\pi \end{aligned} \quad (3.17)$$

Similarly for phase b and c $$f_b(\theta_r) = f_a\left(\theta_r + \frac{2\pi}{3}\right) \quad (3.18)$$

$$f_c(\theta_r) = f_a\left(\theta_r - \frac{2\pi}{3}\right) \quad (3.19)$$

Table 3.3 Trapezoidal Back-Emf as a function of rotor position

θ_r / $f(\theta_r)$	0^o-60^o	60^o-120^o	120^o-180^o	180^o-240^o	240^o-300^o	300^o-360^o
$f_a(\theta_r)$	1	$-\frac{6\theta_r}{\pi} + 3$	-1	-1	$\frac{6\theta_r}{\pi} - 9$	1
$f_b(\theta_r)$	$\frac{6\theta_r}{\pi} - 1$	1	1	$-\frac{6\theta_r}{\pi} + 7$	-1	-1
$f_c(\theta_r)$	-1	-1	$\frac{6\theta_r}{\pi} - 5$		1	$-\frac{6\theta_r}{\pi} + 11$

Similarly the rectangular currents in the stator windings is also a function of rotors' electrical position and is expressed as

$$\begin{aligned} i_a(\theta_r) &= 1 && 0 < \theta_r < \tfrac{\pi}{3}, \tfrac{5\pi}{3} < \theta_r < 2\pi \\ &= 0 && \tfrac{\pi}{3} < \theta_r < \tfrac{2\pi}{3}, \tfrac{4\pi}{3} < \theta_r < \tfrac{5\pi}{3} \\ &= -1 && \tfrac{2\pi}{3} < \theta_r < \tfrac{4\pi}{3} \end{aligned} \quad (3.20)$$

Similarly for phase b and c $$i_b(\theta_r) = i_a\left(\theta_r + \tfrac{2\pi}{3}\right) \quad (3.21)$$

$$i_c(\theta_r) = i_a\left(\theta_r - \tfrac{2\pi}{3}\right) \quad (3.22)$$

Table 3.4 Rectangular Current in PMBLDCM as a function of rotor position

θ_r / $i(\theta_r)$	0^o-60^o	60^o-120^o	120^o-180^o	180^o-240^o	240^o-300^o	300^o-360^o
$i_a(\theta_r)$	1	0	-1	-1	0	1
$i_b(\theta_r)$	0	1	1	0	-1	-1
$i_c(\theta_r)$	-1	-1	0	1	1	0

Table 3.3 and 3.4 summarizes the value of back-emf and corresponding current function respectively.

3.3 MATLAB MODEL OF PERMANENT MAGNET BLDC MOTOR DRIVE

MATLAB models for a PMBLDC motor 3.2 Nm, 540 V, and 3000 Rpm along with rest parameters mentioned in appendix-1 are developed for the operation in different modes. The MATLAB Simulink model in each case is described.

3.3.1 SENSOR BASED OPERATION OF PMBLDC MOTOR

3.3.1.1 Hall SENSORS ANS SPEED/POSITION ENCODER

Hall sensors as well as speed encoder have been used. Hall sensors embedded into the stator placed 120 degree apart. Most BLDC motors have three Hall sensors embedded into the stator on the non-driving end of the motor. Whenever the rotor magnetic poles pass near the Hall sensors, they give a high or low signal, indicating the N or S pole is passing near the sensors.

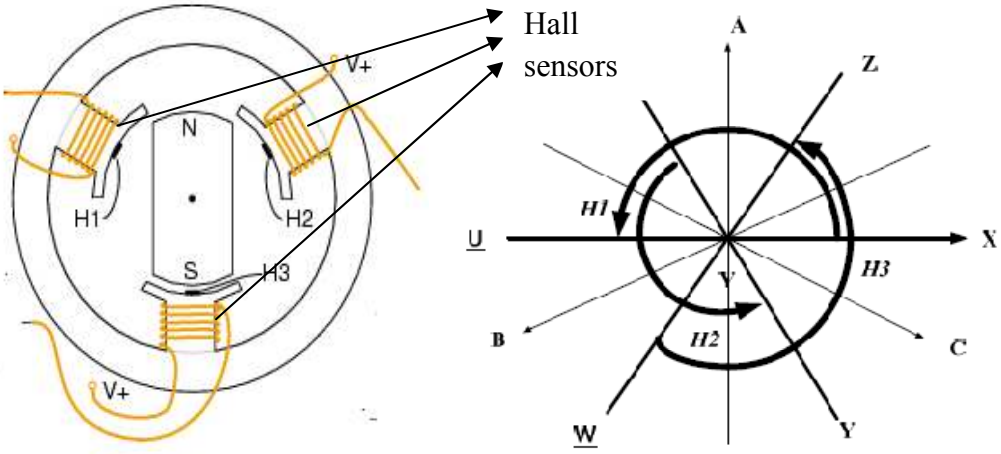

Fig. 3.4: BLDC motor with Hall Sensors on the Stator and their alignment

3.3.1.1.1 PMBLDCM in open loop

In this model PMBLDCM drive operated in open loop mode is being simulated in MATLAB and Simulink model is shown in fig. 3.5.

Based on the combination of these three Hall sensor signals, the exact sequence of commutation is determined. Three signals can result into eight combination out of which six are active and rests two are non-active or called zero vectors. The energizing sequence is listed in table 3.5

Table 3.5 Energizing sequence with Hall Sensors

ha	Hb	hc	Q1	Q2	Q3	Q4	Q5	Q6
0	0	0	0	0	0	0	0	0
0	0	1	0	0	0	1	1	0
0	1	0	0	1	1	0	0	0
0	1	1	0	1	0	0	1	0
1	0	0	1	0	0	0	0	1
1	0	1	1	0	0	1	0	0
1	1	0	0	0	1	0	0	1
1	1	1	0	0	0	0	0	0

In this open loop operation of PMBLDC motor shown in fig. 3.5, there is no control over the current and speed. Only the DC voltage applied to the Inverter decides the magnitude of the speed.

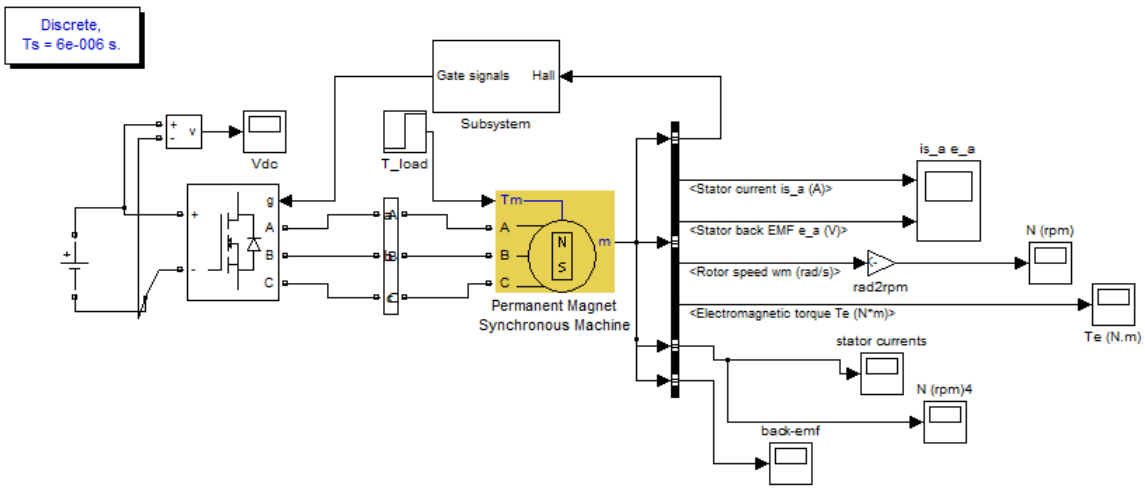

Fig 3.5 Modeling of PMBLDCM in open loop using Hall Sensors

3.3.1.1.2 PMBLDCM in Speed Control Mode (Closed loop operation)

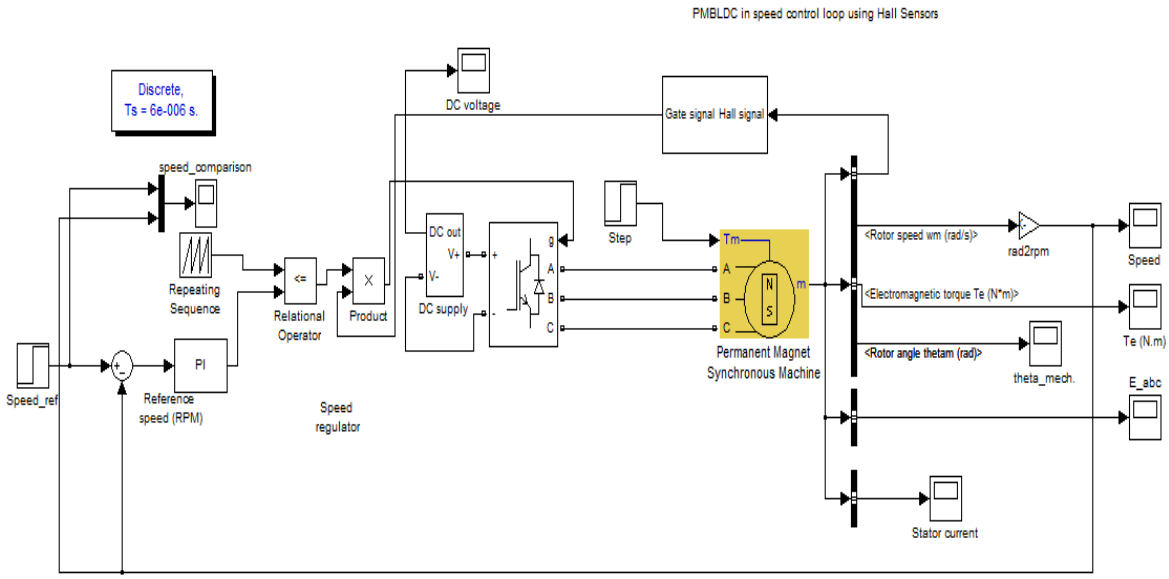

Fig 3.6 Modeling of PMBLDCM in speed control mode using Hall sensor

MATLAB model of PMBDLC drive with speed sensor is shown in fig. 3.6 in closed loop mode. Motor is made to follow the reference speed. The motors' actual speed is measured using speed sensor and processed by the speed controller shown in fig. 3.7.

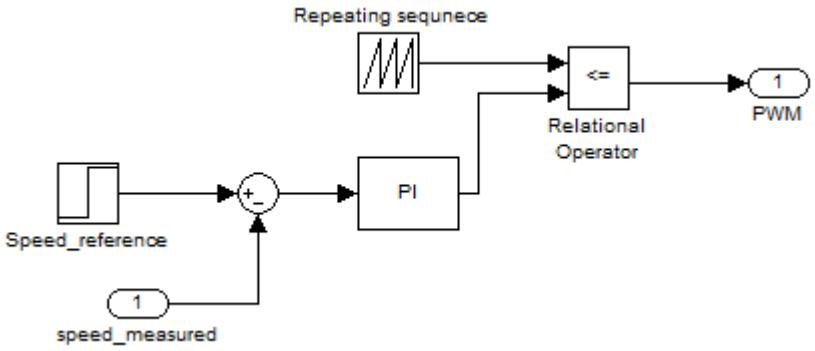

Fig 3.7 Speed PI Controller to generate PWM pulses

The error between the reference speed and measured speed is processed in PI controller and depending upon the magnitude of processed error, the duty ratio of the gate signals to the inverter is changed by the varying width of PWM pulses which is being generated by the

comparing the speed error with the saw tooth wave. Here in the model there is no control over the current.

3.3.1.1.3 PMBLDCM in Speed and Current Control Mode (Closed loop operation)

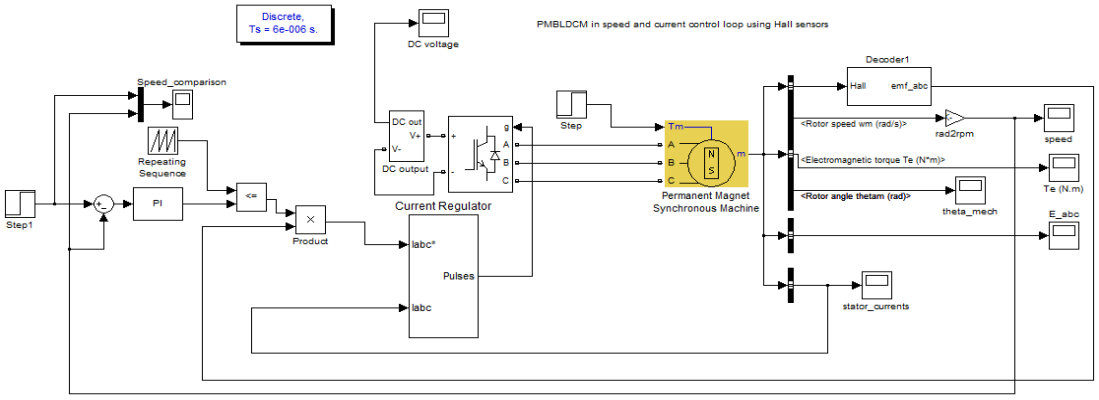

Fig 3.8 Modeling of PMBLDCM in speed and current control mode using Hall Sensors

A MATLAB model of PMBLDCM closed loop mode operation with hall sensors, Speed sensor and speed controller along with current controller is shown in fig 3.8. If there is no control over the current then current shoot up may take place at any time at any value. Therefore to avoid that kind of situations, the current controller block is included in the model fig. 3.8. The performance improvement of this mode of operation is discussed in Chapter 4. Here also, motor is made to follow the reference speed. The error between the reference speed and measured speed is processed in PI controller and depending upon the magnitude of processed error, PWM pulse is generated by the PWM controller. This pulse along with the hall sensor signals will constitute the three phase reference current which when compared with the actual three phase current using the Hysteresis comparator as shown in fig 3.9 would generate the PWM pulses to control the gate triggering of inverter. Hysteresis band is taken to be of width 0.01.

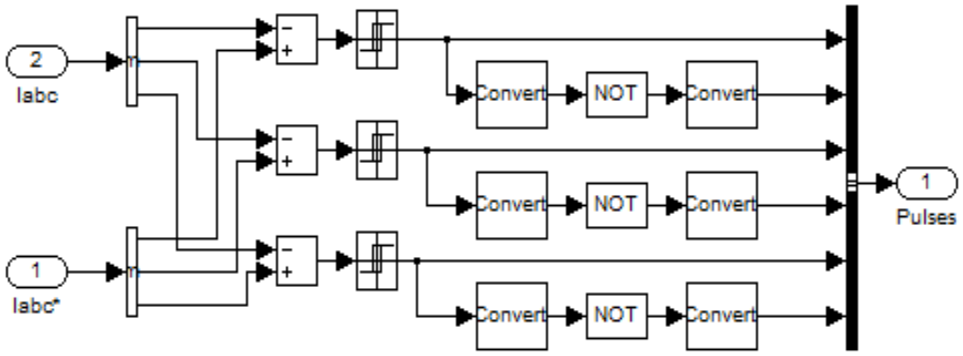

Fig 3.9 Current Hysteresis Controller to generate PWM pulses

3.3.1.2 SPEED SENSOR BASED OPERATION

In this mode of operation the commutation sequence is generated without using the Hall Sensors. Only speed encoder is being used.

3.3.1.2.1 PMBLDCM in Speed Control Mode

It is always desirable either to use less number of sensors or no sensor in a drive as the efficiency of the sensors is affected by the environmental or operating condition, and hence may affect the performance of the drive also. In the earlier models figs 3.5, 3.6 and 3.8, three Hall Effect sensors have been embedded into the stator

.

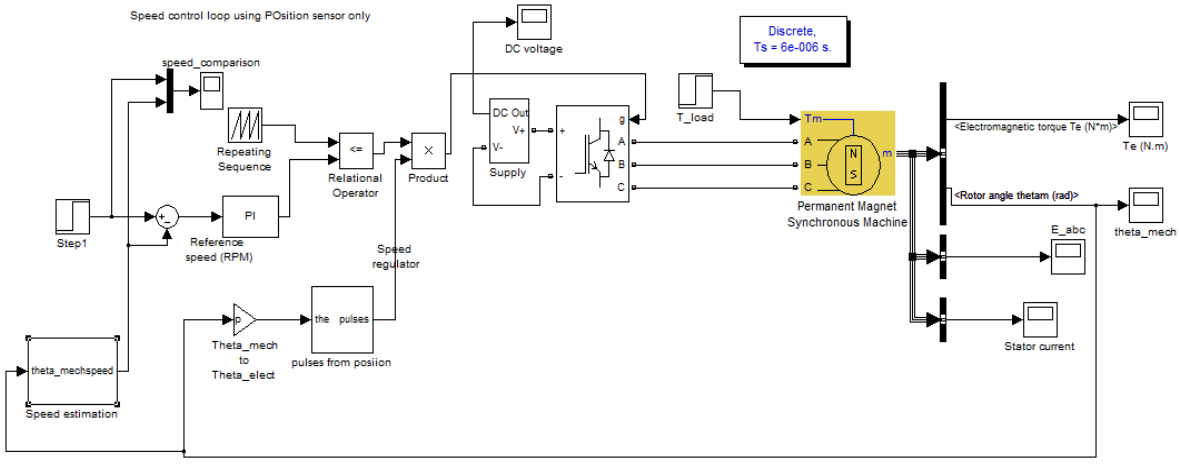

Fig 3.10 Modeling of PMBLDCM in speed control mode using speed/position sensor only

These hall sensors determines the position of the rotor by giving signal a high or low signal, indicating the N or S pole whichever is passing near the sensors. But instead of these three hall sensors, the commutation of PMBLDCM can be carried out with speed encoder or position sensor. Once the speed is known, position of rotor can be calculated and vice versa. Fig. 3.10 shows the MATLAB model of PMBLDC motor drive operated in closed loop mode with speed controller only. Motor is made to follow the reference speed. Here also the error between the reference speed and measured speed is processed in PI controller as shown in fig 3.7 and depending upon the magnitude of processed error, the duty ratio of the gate signals to the inverter is changed which is being generated by the PWM controller. In this mode, there is no control over the current.

3.3.1.2.2 Speed and Current Control of PMBLDCM using Torque Constant

Fig. 3.11 shows a MATLAB model of PMBLDC motor drive operated in closed loop with the speed and current controller. Motor is made to follow the reference speed. The error between the reference speed and measured speed is processed in PI controller as shown in fig 3.7.

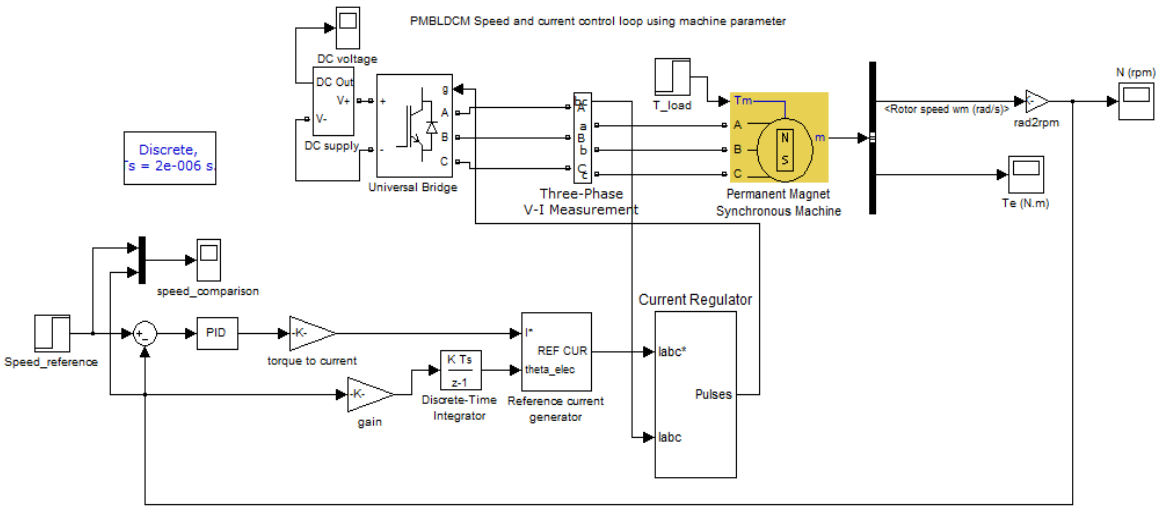

Fig 3.11 Modeling of PMBLDCM in speed and current control mode using Speed sensor only

3.3.1.2.2.1 Speed controller

The reference speed and measured speed is compared and error is processed by PI controller which gives the reference torque as shoe n fig.3.12 and then the reference current magnitude is calculated by using the torque constant of the motor as there is a relation between current and torque of PMBLDCM given by

$$T = K_T I \tag{3.23}$$

Where K_T is the torque constant parameter of the PMBLDC motor (Nm/A).

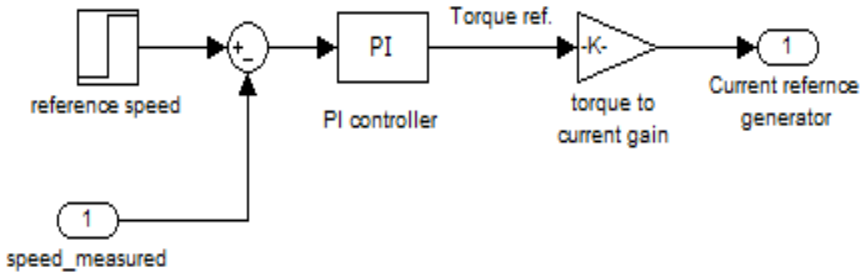

Fig 3.12 Speed Controller to produce Reference current magnitude

3.3.1.2.2.2 Three phase reference current generator

This reference current magnitude calculated from the above equation is then used to calculate three phase reference current which depends upon the value of electrical position of rotor. The three phase reference currents can be computed as per table 3.6:

Table 3.6 Three Phase Reference Current Generator

Rotor electrical position	i_a^*	i_b^*	i_c^*
0-60	I^*	$-I^*$	0
60-120	I^*	0	$-I^*$
120-180	0	I^*	$-I^*$
180-240	$-I^*$	I^*	0
240-300	$-I^*$	0	I^*
300-360	0	$-I^*$	I^*

3.3.1.2.2.3 Hysteresis Comparator

In hysteresis comparator as shown in fig 3.9, the actual current is compared with the reference value and the value of this error is passed to hysteresis band. The pulse output of hysteresis block is fed to the gate of the inverter module as the gate pulses for switching such that the drive could follow the reference speed trajectory and the current also does not exceed its rated value.

3.3.2 SENSORLESS OPERATION OF PMBLDC MOTORS

In this mode of operation, the motors' parameters and current status of voltages and currents is being used to carry out the commutation.

In all the previous mentioned schemes, sensors are being used either the hall sensors or speed encoder or position sensor. But it would be quite effective for the drive operation in dusty, oily or sluggish environments if there is no sensor. No sensors mean the estimation of speed or rotor's position from its voltages, currents and motors' parameter.

Fig. 3.13 shows the sensorless operation of the PMLDC motor. Here the motor is operated in the speed and current control mode.

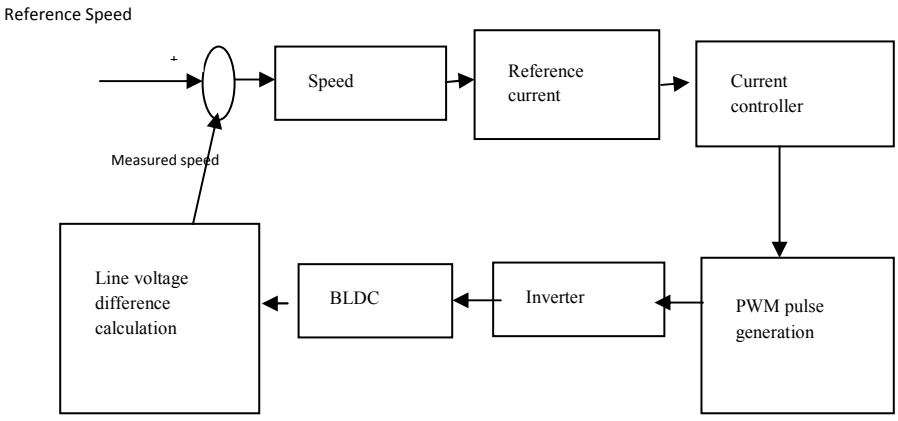

Fig 3.13 Block Diagram of the Sensorless Scheme

Speed and Back-Emf estimation from the line voltages

Using equations 3.6, 3.7 and 3.8 the phase voltages are expressed as

$$V_{an} - V_{bn} = V_{ab} = R(i_a - i_b) + (L_s - M)\frac{d}{dt}(i_a - i_b) + e_a - e_b \quad (3.24)$$

$$V_{bn} - V_{cn} = V_{bc} = R(i_b - i_c) + (L_s - M)\frac{d}{dt}(i_b - i_c) + e_b - e_c \quad (3.25)$$

$$V_{cn} - V_{an} = V_{ca} = R(i_c - i_a) + (L_s - M)\frac{d}{dt}(i_c - i_a) + e_c - e_a \quad (3.26)$$

Assuming $(L_s - M) = L$ and $(i_a + i_b + i_c = 0)$ because of STAR or Y connection of stator then, subtracting (3.22) from (3.21), (3.22) from (3.23) and (3.21) from (3.23) we have,

$$V_{ab} - V_{bc} = V_{abbc} = R(-3 * i_b) + L\frac{d}{dt}(-3 * i_b) + e_a + e_c - 2 * e_b \quad (3.27)$$

$$V_{bc} - V_{ca} = V_{bcca} = R(-3 * i_c) + L\frac{d}{dt}(-3 * i_c) + e_a + e_b - 2 * e_c \quad (3.28)$$

$$V_{ca} - V_{ab} = V_{caab} = R(-3 * i_a) + L\frac{d}{dt}(-3 * i_a) + e_c + e_b - 2 * e_a \quad (3.29)$$

From above (3.24), (3.25) and (3.26) equations, we have

$$V_{abbc} = R(-3 * i_b) + L\frac{d}{dt}(-3 * i_b) + e_a + e_c - 2 * e_b \quad (3.30)$$

$$V_{bcca} = R(-3 * i_c) + L\frac{d}{dt}(-3 * i_c) + e_a + e_b - 2 * e_c \quad (3.31)$$

$$V_{caab} = R(-3 * i_a) + L\frac{d}{dt}(-3 * i_a) + e_c + e_b - 2 * e_a \quad (3.32)$$

At the commutation instant of phase B as shown in shaded area in fig 3.14

$$i_a = -i_c \text{ And } i_b = 0 \quad (3.33)$$

Also $$e_a = -e_c \quad (3.34)$$

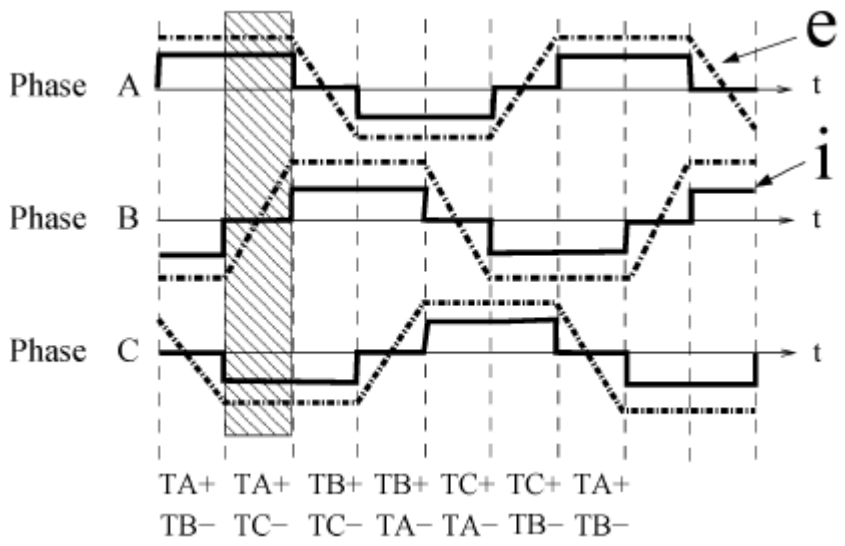

Fig 3.14 Trapezoidal Back-emfs and Rectangular Current waveforms of three-phase

Substituting equations (3.30) and (3.31) in (3.27) we get,

$$V_{abbc} = -2 * e_b \tag{3.35}$$

Thus during the commutation of phase B, V_{abbc} gives the back-emf of phase inverted and twice of actual magnitude. Similarly during the commutation of phase A and C, V_{caab}, V_{bcca} would provide the phase A and C back-emfs.

$$V_{bcca} = -2 * e_c \tag{3.36}$$

$$V_{caab} = -2 * e_a \tag{3.37}$$

Now this back-emf estimated can be analyzed to carry out the commutation.

Whene_a, e_b and e_c are available from (3.35, 3.36 and 3.37) then speed of motor can be calculated by the motors' available parameter i.e. back emf constantK_B.

$$E = K_B \omega_e \tag{3.38}$$

where K_B is the back-emf constant which for the motor taken in the present analysis is

K_B=136.1357 V_peakL-L/krpm (3.39)

Or 0.1361357 V_peakL-L/rpm

and ω_e is the electrical rotor speed in rad/s. The back-emf increases with motor speed and is constant when the speed is constant. So this E is taken as the

$$\text{E} = \textbf{max ([}e_a\textbf{, }e_b\textbf{ and }e_c\textbf{])}. \tag{3.40}$$

The relation between electrical and mechanical speed is given by

$$\omega_e = \frac{P}{2}\omega_m = p * \omega_m \tag{3.41}$$

Where ω_e is electrical speed and ω_m is the mechanical speed of rotor, p is the number of pole pairs and P is the total number of poles.

Once the speed is obtained then the same speed controller as shown in fig 3.17 is used to get the current reference magnitude and then the hysteresis comparator as shown in fig 3.9 can be used to control the commutation circuit. Thus the pulses obtained from the hysteresis comparator are given to the inverter so that motor can follow the reference speed without exceeding the rated current value.

3.3.2.1 BACK-EMF AND SPEED CONTROLLER BASED OPERATION OF PMBLDCM

Back-Emf estimated from line voltages in above equation is now checked for its polarity. One advantage of this method is that high speed operation can be done as the back-emf magnitude is low at low speeds. But no such issue if polarity is checked.

3.3.2.1.1 PMBLDCM in Speed Control Mode with 120 degree commutation

In this mode of operation the dependence of back-emf on the rotor position is taken into consideration. So the rotor position can be known from the back-emf waveform characteristic. The back-emf of the three phases is 120 electrical degree phase shifted from each other. This technique considers the polarity of the three phase-back-emf and helps in commutation. When the BLDCM is driven with 120-degree commutation, it is two phases "on" and the other phase floating, as shown in Fig 3.15. In every commutation step, one phase winding is connected to positive supply voltage, one phase winding is connected to negative supply voltage and one phase is floating. The back-EMF in the floating phase will result in a "zero crossing" when it crosses the average of the positive and negative supply voltage.

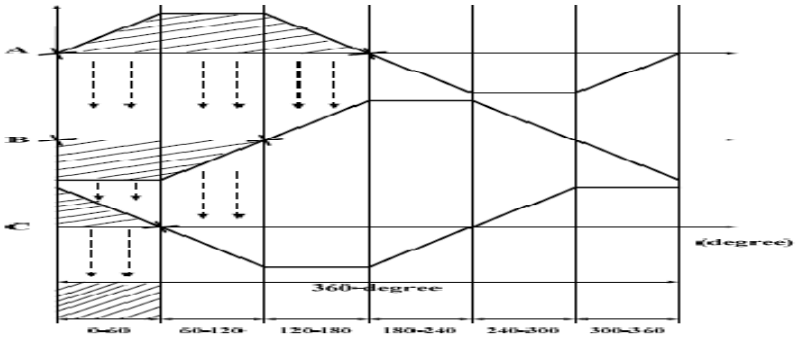

Fig 3.15 Trapezoidal Back-emf of three phases

Depending upon the polarity of back-emf either positive or negative, the switching pulses to the inverter is given so as to result in the drive motion properly. Table 3.7 lists the switching pulse "on" given to which of the IGBT/diode switch depending on the polarity of the back-emf.

Table 3.7 Switching sequence of the Inverter with 120 degree commutation

Interval	IGBT/Diode switch "on"	Polarities of e_a, e_b and e_c		
		A	B	C
0-60	Q1 , Q6	+	0	-
60-120	Q3, Q6	0	+	-
120-180	Q3, Q2	-	+	0
180-240	Q5, Q2	-	0	+
240-300	Q5, Q4	0	-	+
300-360	Q1, Q4	+	-	0

Fig 3.16 shows a MATLAB model of PMBLCM simulated for the 120 degree commutation.

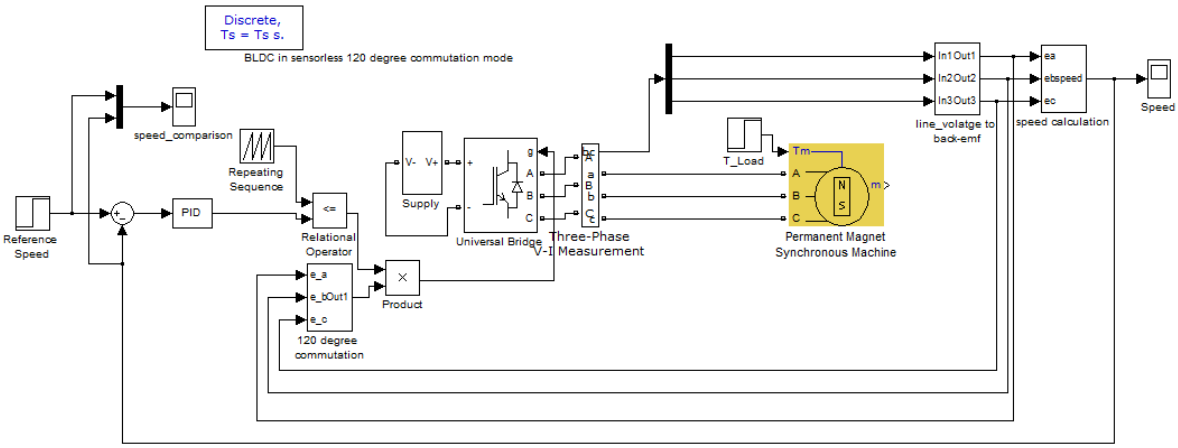

Fig 3.16 Modeling of PMBLDCM in speed control mode with 120 degree commutation with no sensor

Fig. 3.16 shows the PMBLDC motor drive operated in closed loop with speed controller only. Motor is made to follow the reference speed. Here also the error between the reference speed and measured speed is processed in PI controller as shown in fig 3.7 and depending upon the magnitude of processed error and switching "on" pulse form 120 degree commutation circuitry, the duty ratio of the gate signals to the inverter is changed But instead of using three hall sensors, one position is employed. Here there is no control over the current.

3.3.2.1.2 PMBLDCM in Speed Control Mode with 180 degree commutation

BLDCM earlier driven with 120-degree commutation scheme is two phases "on" and the other phase floating, Due to the reason that torque production is almost directly proportional to the phase current, the floating phase doesn't produce any torque. The 180-degree commutation scheme can generate larger output torque than 120- degree for the same given power supply because all the three phase are "on" in each conduction intervals of 180-degree.

Here also the polarity of back-emf waveform is checked but for duration of 180 degree hence scheme called "180 degree commutation". Depending upon the polarity of back-emf either positive or negative, the switching pulses to the inverter is given so as to result in the

drive motion properly. Table 3.8 lists the switching pulse "on" given to which of the IGBT/diode switch depending on the polarity of the back-emf as shown on fig 3.14.

Table 3.8 Switching sequence of the Inverter with 180 degree commutation

Interval	IGBT/Diode switch "on"	Polarities of e_a, e_b and e_c		
		A	B	C
0-60	Q1 , Q4 , Q5	+	-	+
60-120	Q1, Q4 , Q6	+	-	-
120-180	Q1, Q3 , Q6	+	+	-
180-240	Q2, Q3 , Q6	-	+	-
240-300	Q2, Q3 , Q5	-	+	+
300-360	Q2, Q4 , Q5	-	-	+

Fig.3.17 shows a MATLAB model of PMBLCM simulated for the 180 degree commutation.

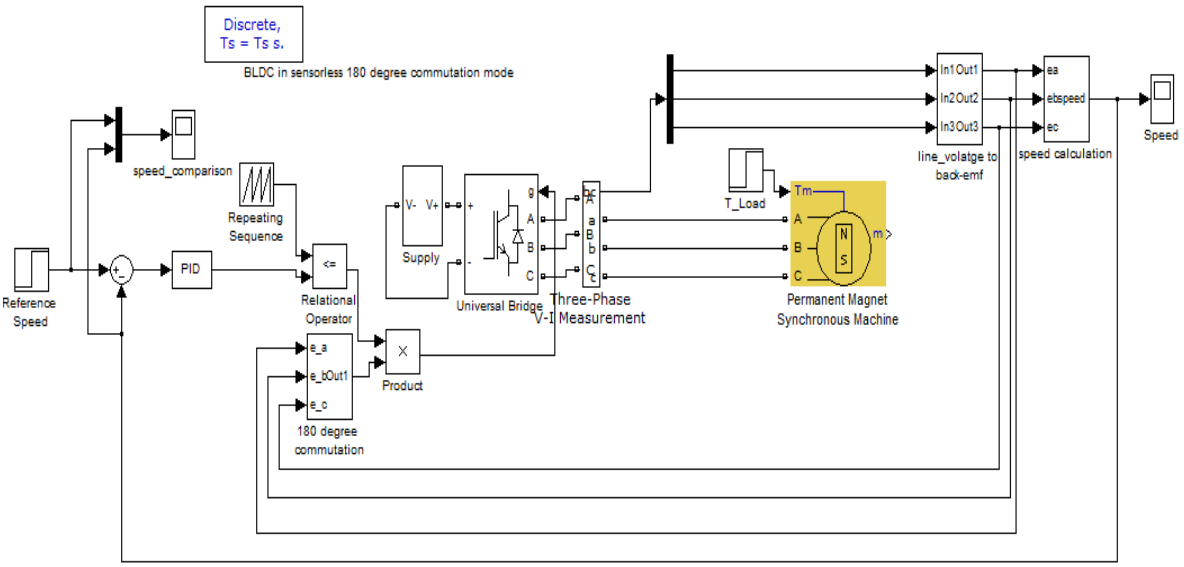

Fig 3.17 Modeling of PMBLDCM in speed control mode with 180 degree commutation with no sensor

In this mode, PMBLDC motor drive is operated in closed loop with speed controller only. Motor is made to follow the reference speed. Here also the error between the reference speed and measured speed is processed in PI controller as shown in fig 3.7 and depending upon the magnitude of processed error and switching "on" pulse form 180 degree commutation circuitry, the duty ratio of the gate signals to the inverter is changed which is being generated by the PWM controller. But instead of using three hall sensors, one position is employed. Here there is no control over the current.

3.3.2.2 PMBLDCM in Speed and Current control mode

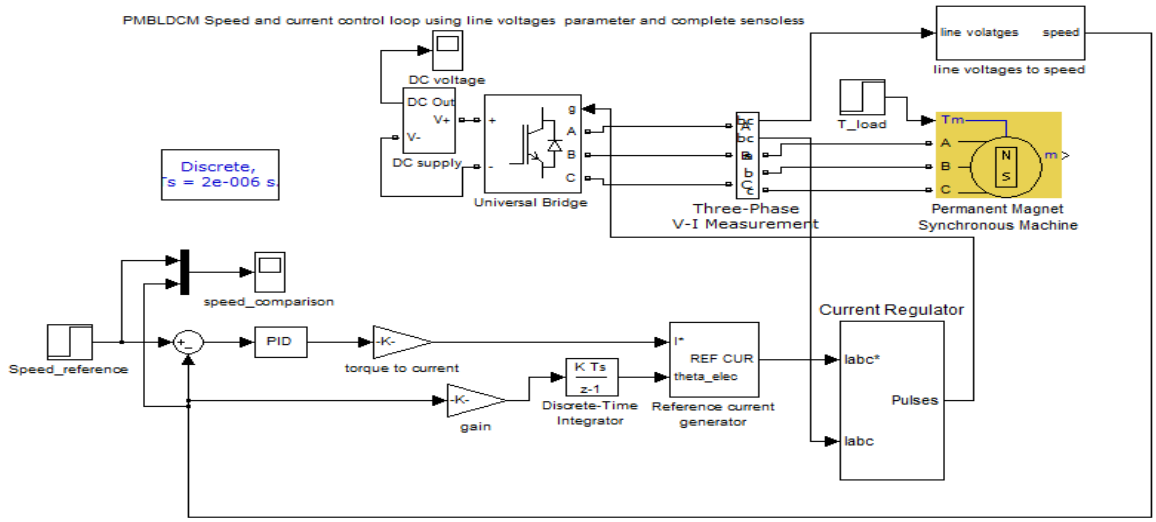

Fig 3.18 Speed and current Control mode with No Sensors

Fig. 3.18 shows the sensorless operation of the brushless motor while estimating the speed from the line voltage difference which is further filtered and the filtered line voltage gives the back-emf at the commutation instants as in equation (3.35, 3.36 and 3.37).

3.3.3 FUZZY LOGIC CONTROLLER BASED SPEED AND CURRENT CONTROL OF PMBLDCM USING POSITION/SPEED SENSOR

Fuzzy logic is an innovative technology that enhances conventional system design with engineering expertise. One can circumvent the need for rigorous mathematical modeling with the use of the fuzzy logic. Unlike the reasoning based on classical logic, fuzzy reasoning aims at the modeling of reasoning schemes based on uncertain or imprecise information. The past several years have witnessed a rapid growth in the number and variety of applications of fuzzy logic. The most visible applications are in the realms of consumer products, intelligent control and industrial systems. Less visible, but of growing importance, are applications relating to data processing, fault diagnosis, man-machine interfaces, quality control and decision support systems. Although fuzzy logic has been and still is controversial to some extent, its successes are now too obvious to be denied

In model fig. 3.20, PMBLDC motor drive is operated in closed loop. Motor is made to follow the reference speed. The difference here lies in the fact that the error between the reference speed and measured speed is processed in Fuzzy Logic Controller. The output of this FLC controller output is the reference torque which is then used to estimate the reference current magnitude using the torque constant of the motor. Using this reference current three phase reference current is generated and compared with the actual current flowing using the Hysteresis comparator shown in fig 3.9.

Fuzzy Logic Speed Controller

The block diagram show in fig 3.21 gives the idea of how the fuzzy control is implemented. The FLC does not require a mathematical model of the system and it works on a structure prepared from the knowledge base.

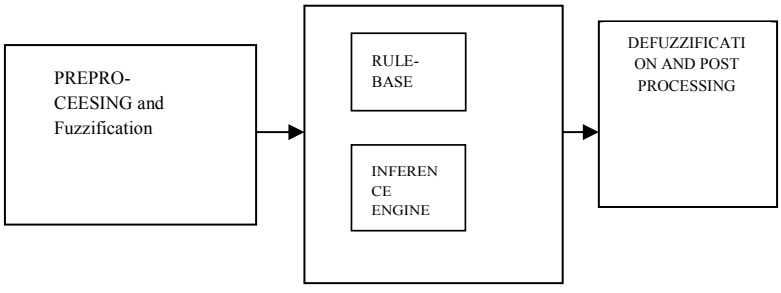

Fig. 3.19 Fuzzy Logic Controller

The description of FLC scheme used in this investigation is as follows:

(a) Fuzzification: The first block inside the controller is Fuzzification, which is a look-up in the membership function to derive the membership grade. The membership function (also known as degree of belonging) is in the range of 0 to 1.

(b) Rules base: A rule allows for several variables both in the premise and the conclusion. A linguistic controller used here contains rules in the "if-then" format. These rules are imprecise and expressed in terms of linguistic variable. The Rule Base used for the Fuzzy Logic Speed controller used is shown in table 3.9. The fuzzy members chosen are: Zero: ZO, Positive Big: PB, Positive Small: PS, Negative Big: NB, Negative Small: NS. In Fuzzy Logic Speed controller the inputs used are the speed error and rate of change of speed error The fuzzy logic control output i.e. the torque is a function of $\Delta\,\omega$ (speed error) and $\Delta\,\omega'$ (change of speed error) and is expressed as $T = FLC(\Delta\,\omega', \Delta\,\omega)$. The triangular shaped membership function has been chosen due to the resulting best control performance and simplicity. The height of the membership functions in this case is one for all. Some degree of overlap is provided for neighboring fuzzy subsets. Here a Fuzzy logic controller (FLC) is being used to estimate the torque using "if-then" rule on the speed error and rate of change of error as per table shown below.

(c) Defuzzification: The reverse of Fuzzification is called Defuzzification: The rules of FLC produce required output in a linguistic variable. Linguistic variables have to be transformed to crisp output. By using the center of gravity "centroid" defuzzification method, crisp output is obtained. The output of the Fuzzy Logic speed controller is torque.

Table 3.9 Fuzzy Logic Rule Base Table

$\Delta\,\omega$ ' / ω	NB	NS	ZO	PS	PB
NB	NB	NB	NB	NS	ZO
NS	NB	NS	NS	ZO	PS
ZO	NB	NS	ZO	PS	PB
PS	NS	ZO	PS	PS	PB
PB	ZO	PS	PB	PB	PB

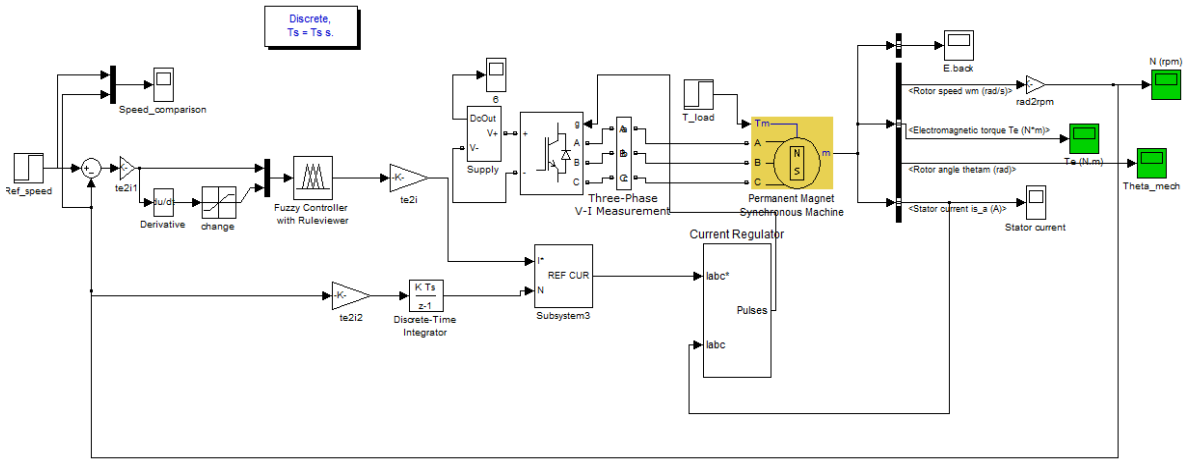

Fig 3.20 Modeling of PMBLDM Using FLC speed controller and Current Hysteresis Controller

Fig. 3.20 shows the model of the PMBLDCM operation in speed and current control mode using the Fuzzy logic based speed controller and Hysteresis current controller. The rule based used for the Fuzzy logic based speed controller is shown in table 3.9.

3.4 CONCLUSION

The Simulation models for the different mode of operation for the sensor based and sensorless drive have been presented in this chapter. The sensor based drive is simulated in open loop, with speed controller and with both speed and current controllers. PI and FLC speed controllers are used for tracking the reference speed and hysteresis controller for current control. The sensor-less drive is simulated using phase-to-phase voltages difference scheme using the theoretical result that the line voltage difference when filtered gives the back emf that is reverse in phase and twice of the actual back-emf amplitude. Thus all the schemes implemented in this work are modeled in this chapter along with their mathematical equations.

CHAPTER IV
SIMULATION RESULTS AND ANALYSIS

4.0 GENERAL

Simulations have been carried out in the previous chapter and results are shown here for sensor based and sensorless based PMBLDC motor drive.

4.1 SIMULATION RESULTS

Through the simulation results, the performance of the PMBLDC motor is studied here under various operating conditions like operation at a particular reference speed, change of reference speed, sudden application of load. Some work performed with sensors. But sensors reduce the reliability of the operation of the motor in the sluggish environment. So a sensorless scheme is also implemented.

4.2 SENSOR BASED OPERATION OF PMBLDCM

4.2.1 Performance of PMBLDCM with Hall Sensors and Speed/Position encoder

4.2.1.1 Simulation result of PMBLDCM in open loop mode

Fig. 4.1 shows the performance of the PMBLDC motor drive in open loop mode. Hall Effect sensors are used in this scheme which are embedded in to the stator and placed 120 degree apart. The motor is not given any instruction. Only the dc input voltage applied to inverter decides the magnitude of speed of its operation. In this work a DC voltage of 200 V is applied and a sudden load of 1Nm at 0.1 seconds.

It is observed from speed response in fig. 4.1 that on sudden application of load at instant of 0.1seconds, the speed of motor falls by a large value as no control over speed. Starting torque in this scheme is high which is desirable. As in this scheme there is no control over the drive so it is observed that at starting, the motor line current is very high of magnitude 5A. High starting is no desirable. Though it is not exceeding the rated value but can cause harm to the windings and personnel too.

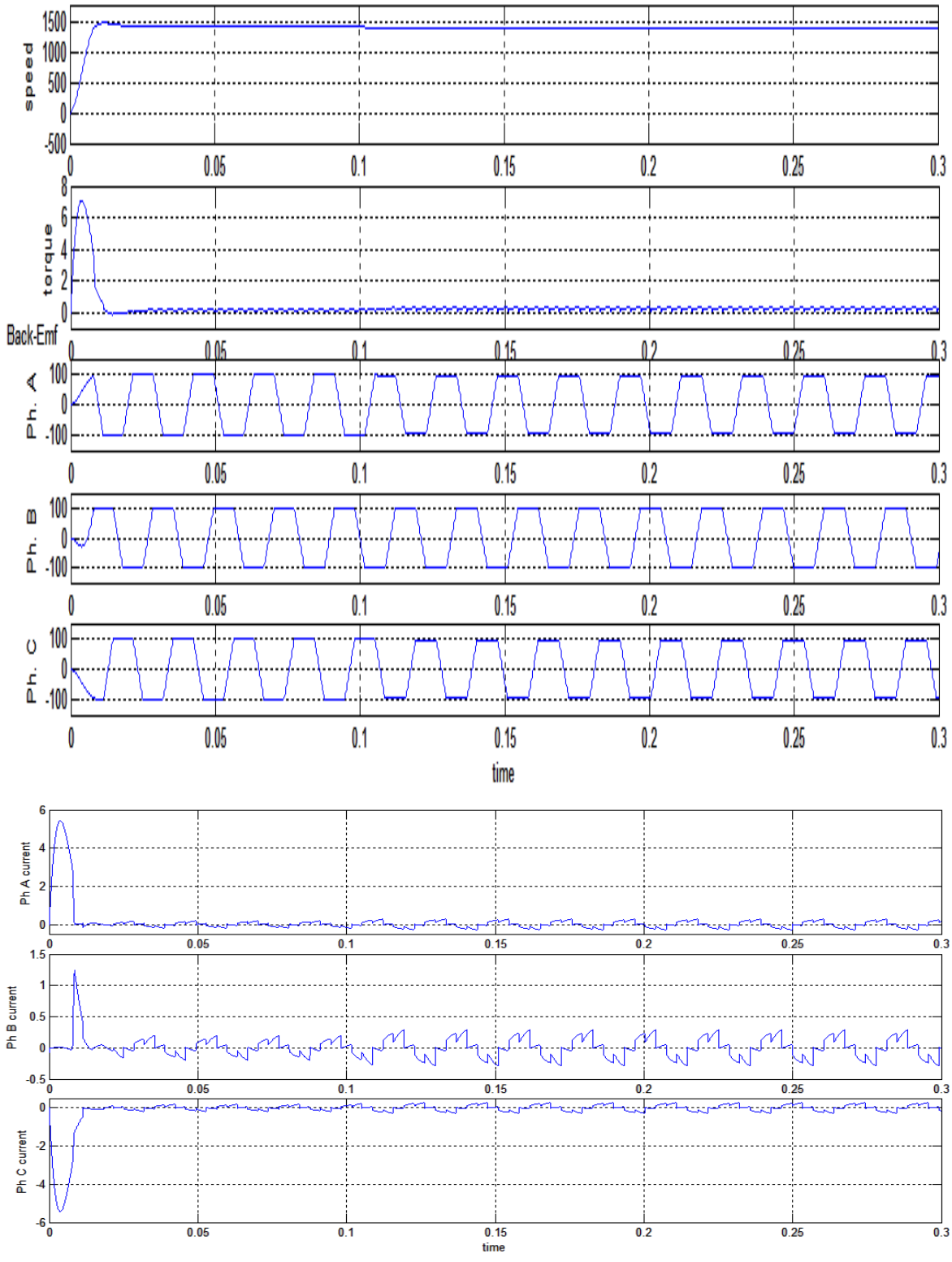

Fig 4.1 Performance of the PMBLDC motor drive in open loop using Hall sensors

It is also observed from the current response that the current is somewhat near to the rectangular shape which is its nature due to the trapezoidal back-emf wave pattern and desirable constant torque.

As per table 3.3 there are six active (non-zero switching signals) and two zero switching signals (000, 111). Fig 4.2.Shows the switching sequence for three phase bridge inverter. These six signals are created in such a way that in each cycle, every switch conducts for 120 degree, then commutates for 60 degree and then its negative phase conduction takes place for another 120 degree and then this negative phase switch gets commutated for 60 degree.

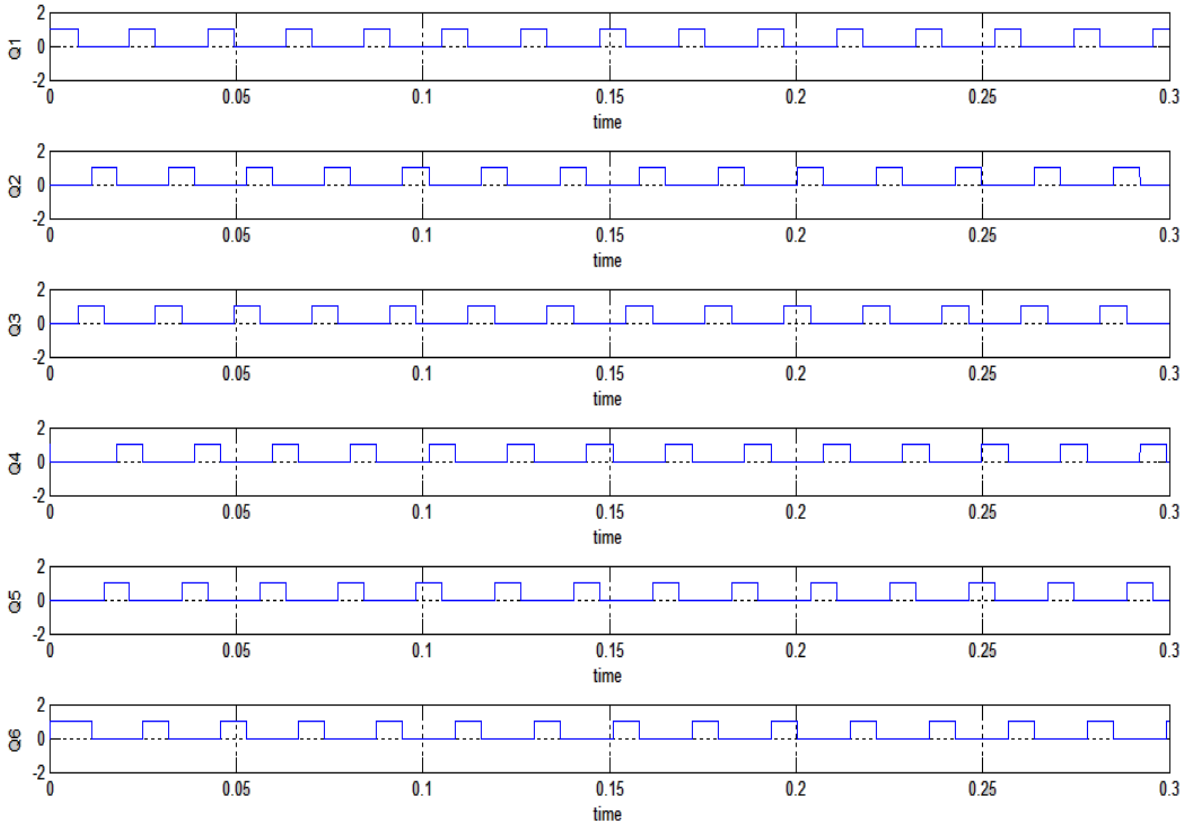

Fig 4.2 Switching sequence for Inverter based on the Three Hall Effect Sensors

The three Hall Effect sensors give six switching pulses for the inverter. When these pulses are given to the inverter, it supplies the voltage to that phase for duration equal to its pulse width.

4.2.1.2 Simulation result of PMBLDCM in speed control mode

Fig. 4.3 shows the performance of the PMBLDC drive with PI speed controller only with K_p= 0.080 and K_i=0.0000001. The motor is running at the reference speed of 1000 RPM up to 0.2 seconds which is then changed to 1500 RPM.

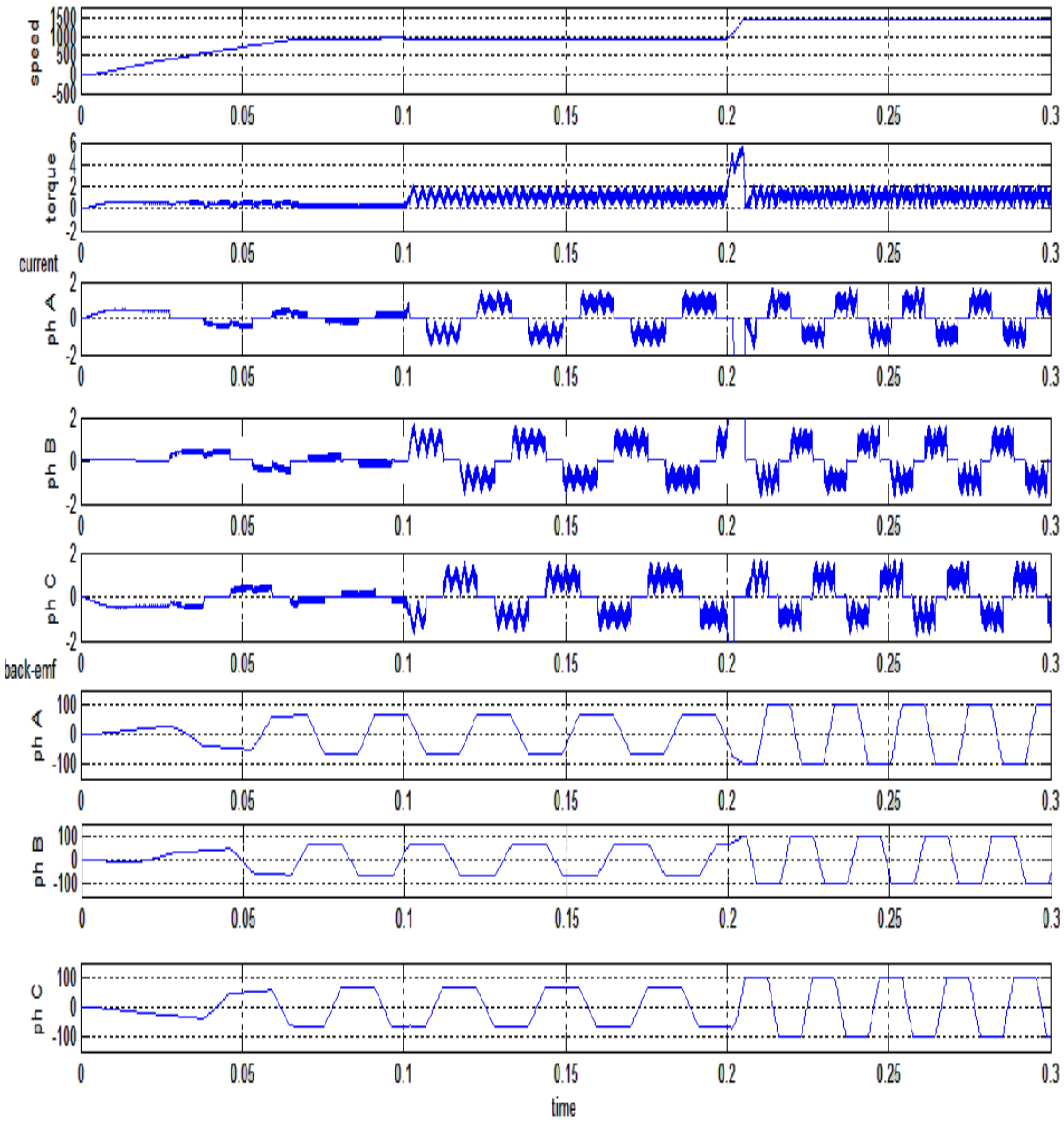

Fig 4.3 Performance of the PMBLDC motor in speed control mode using Hall sensors

From the speed response shown in figure 4.3 it is observed that the motor takes about 0.007319 seconds to reach the initial reference speed of 1000 RPM.

From the torque response, it is observed that there are large ripples in it as there is no control over the current and torque depends on it and also at instant when there is change in reference speed, the electromagnetic torque rises instantaneously because the motor draws a large amount of current. It is clearly observed from current waveform.

Switching for the inverter using the hall sensors will be the same as it was in the case without speed sensor (i.e. in open loop operation).

Also the sudden application of the load of 1 Nm at 0.1 seconds on the motor did not result in a noticeable dip in motor speed. However during the load perturbation the value of current increases from about 0.5426 A to about 0.7867 A. It is also seen that the current is somewhat near to the rectangular shape which is its nature due to the trapezoidal back-emf pattern and desirable constant torque. Another point observed is that when the reference speed is changed from 1000 RPM to 1500 RPM then though the current ratings are not exceeded but there is a quick change in the current values which are of high magnitude comparing to the earlier instant of time (near about from 0.7867A to 4.052 A) This is because there is no control over the currents.

It is observed from the back-emf waveform of the PMBLDC motor in the scheme that it is increasing with the increasing speed and becomes constant when the speed is constant. Also at time, t=0.2 seconds when the speed increases then correspondingly back-emf also increases. It means it follows the relation that back-emf is directly proportional to speed

4.2.1.3 Simulation result of PMBLDCM in Speed and Current Control Mode

Fig. 4.4 show the performance of the Hall sensor-based commutation of PMBLDC motor drive with PI speed controller (K_p= 1.2 and K_i=0.3) and current hysteresis controller. The motor is running at the reference speed of 1000 RPM up to 0.2 seconds which is then changed to 1500 RPM.

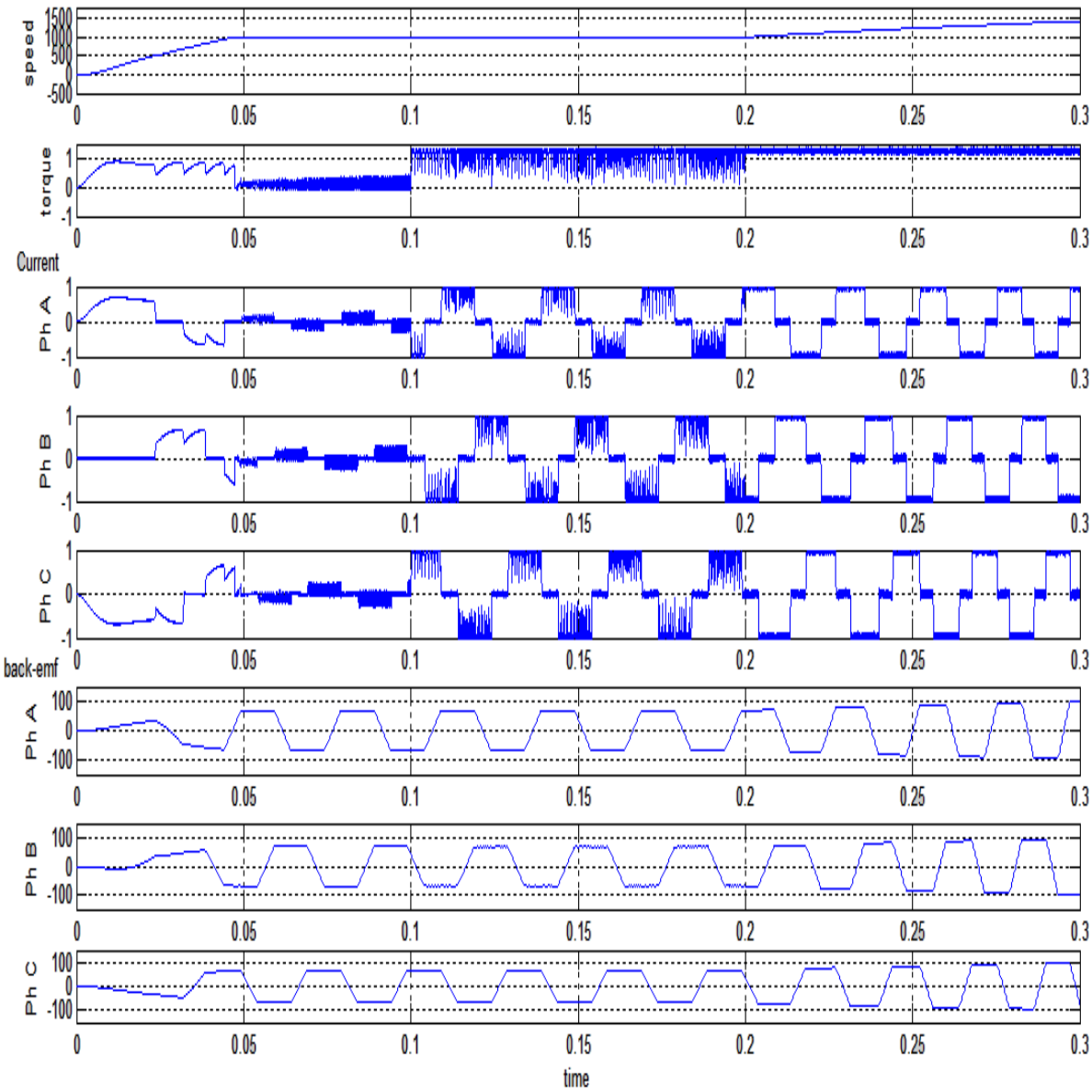

Fig 4.4 Performance of the PMBLDC motor in speed and current control mode using Hall sensors

From the speed performance in figure 4.4 it is observed that the motor takes 0.04723 seconds to reach the initial reference speed of 1000 RPM. Also the sudden application of the load of 1 Nm at 0.1 seconds on the motor did not cause a noticeable dip in motor speed.

From the torque response, it is observed that when the load is applied, there are not large ripples in torque as there is control over the current and torque depends on it and also at instant when there is change in reference speed, the electromagnetic torque remains approximately the same to support the load torque. Also, here the starting torque produced by the motor is approx 0.8541Nm. Initially the torque ripples are confined to 0.5Nm and after its start, to about 1.2Nm.

It is observed from the current response that the starting current drawn by the motor is near about 0.6892A. During the load perturbation i.e. at the instant 0.1 seconds at which a sudden load of 1Nm is applied on motor shaft, the value of current is increased compared to the no-load current. After the load is applied the motor is drawing a current of 1.03 A which is not a large value. Thus, it is safer for the windings as well as the for the operator personnel. The current drawn by the motor is also much closer to the rectangular shape which is its nature due to the trapezoidal back-emf pattern and desirable constant torque. Another reason is the current control loop. It is observed that when the reference speed is changed from 1000 RPM to 1500 RPM then there is only a small change in the current values which was large in the previous case where there is no control over the currents. So the scheme with speed and current controller is better that the one with speed control only.

It is observed from back-emf waveform that it increases with the increasing speed and becomes constant when the speed is constant. Also at time, t=0.2 seconds when the speed increases then correspondingly back-emf also increases. It means follow the relation that back-emf is directly proportional to speed.

4.2.2 Performance of PMBLDCM with Speed/Position Sensor Only

4.2.2.1 Simulation result of PMBLDCM in Speed control mode

Fig. 4.5 shows the performance of the PMBLDC motor drive when only speed sensor is used. The speed error processed by PI speed controller with K_p= 0.8 and K_i=0.0007. The motor is running at the reference speed of 1000 RPM up to 0.2 seconds which is then changed to 1500 RPM.

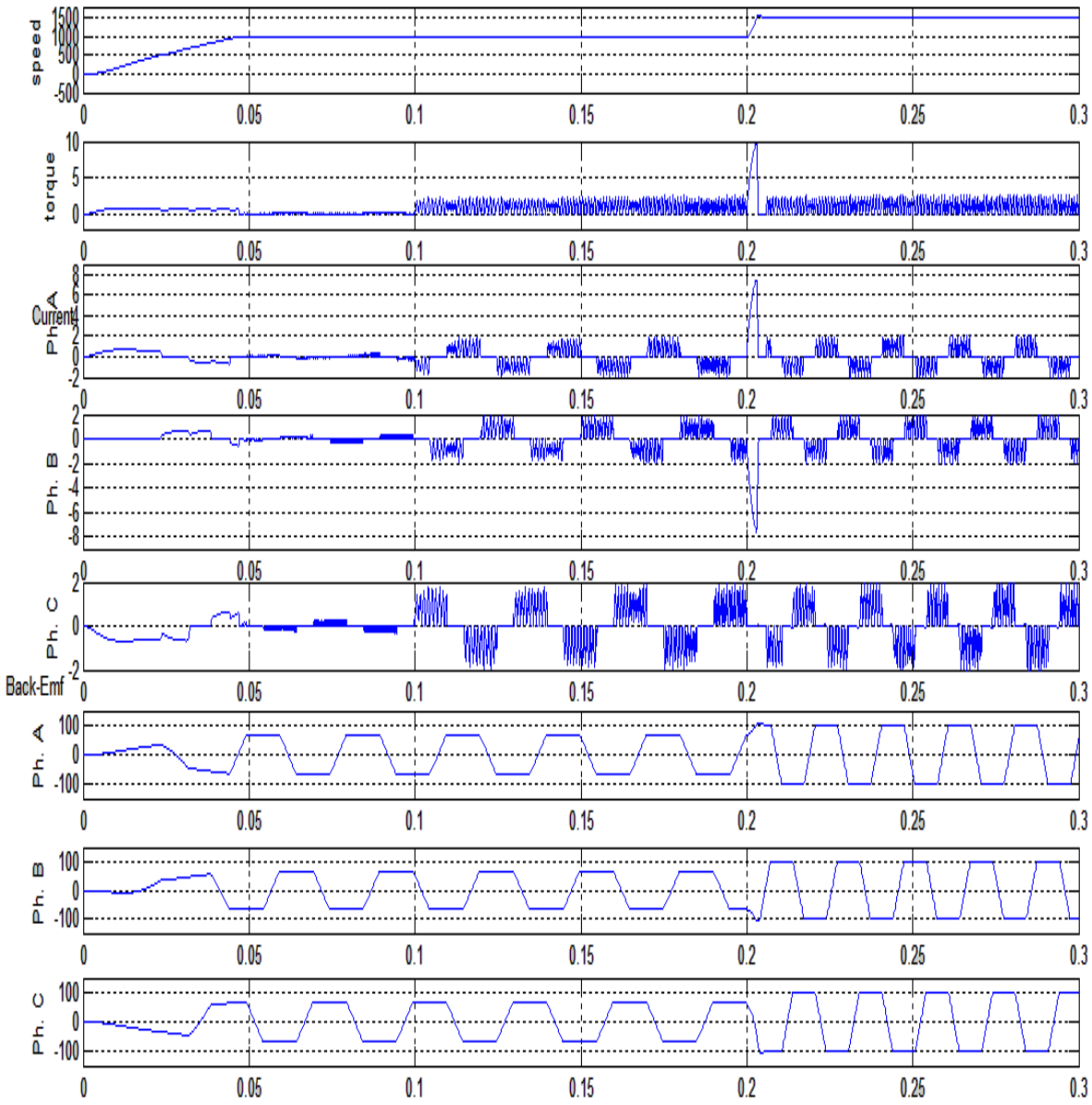

Fig 4.5 Performance of the PMBLDC motor in speed control mode using Speed sensor only

From the speed performance in figure 4.5 it is observed that the motor takes about 0.04589 seconds to reach the initial reference speed of 1000 Rpm. Also the sudden application of the load of 1 Nm at 0.1 seconds on the motor did not cause a noticeable dip in motor speed. When the reference speed is changed to 1500 Rpm at instant t=0.2 seconds, then an overshoot of 70 Rpm in speed can be observed.

From the torque response, it is observed that when the load is applied, there are large ripples in torque as there is no control over the current and torque depends on it and also at instant when there is change in reference speed, the electromagnetic torque suddenly rises to a value 8.83Nm. Also here the starting torque produced is 0.8Nm.

It is observed from the current performance that the starting current drawn by the motor is 0.5204A. During the load perturbation i.e. at the instant 0.1 seconds at which a sudden load of 1Nm is applied on motor shaft, the value of current is increased compared to the no-load current. After the load is applied the motor is drawing a current of 1.87 A. The current drawn by the motor is also much closer to the rectangular shape but large variation in its magnitude. It is observed that when the reference speed is changed from 1000 RPM to 1500 RPM then there is only a large overshoot in the current values, from 1.87A to 7.618A. This value of current is very high and close to the current rating. This is due to absence of current controller which could otherwise limit this value. Here also, the current behavior is similar to the rectangular one but the fluctuation is also large.

It is observed from back-emf waveform that it increases with the increasing speed and becomes constant when the speed is constant. Also at time, t=0.2 seconds when the speed increases then correspondingly back-emf also increases. It means follow the relation that back-emf is directly proportional to speed.

4.2.2.2 Simulation result of PMBLDCM in Speed and Current Control Mode

Fig. 4.6 show the performance of the PMBLDC motor drive with PI speed controller (K_p=2 and K_i=0.8) and current hysteresis controller when only speed sensor is used. The motor is running at the reference speed of 1000 RPM up to 0.2 seconds which is then changed to 1500 RPM.

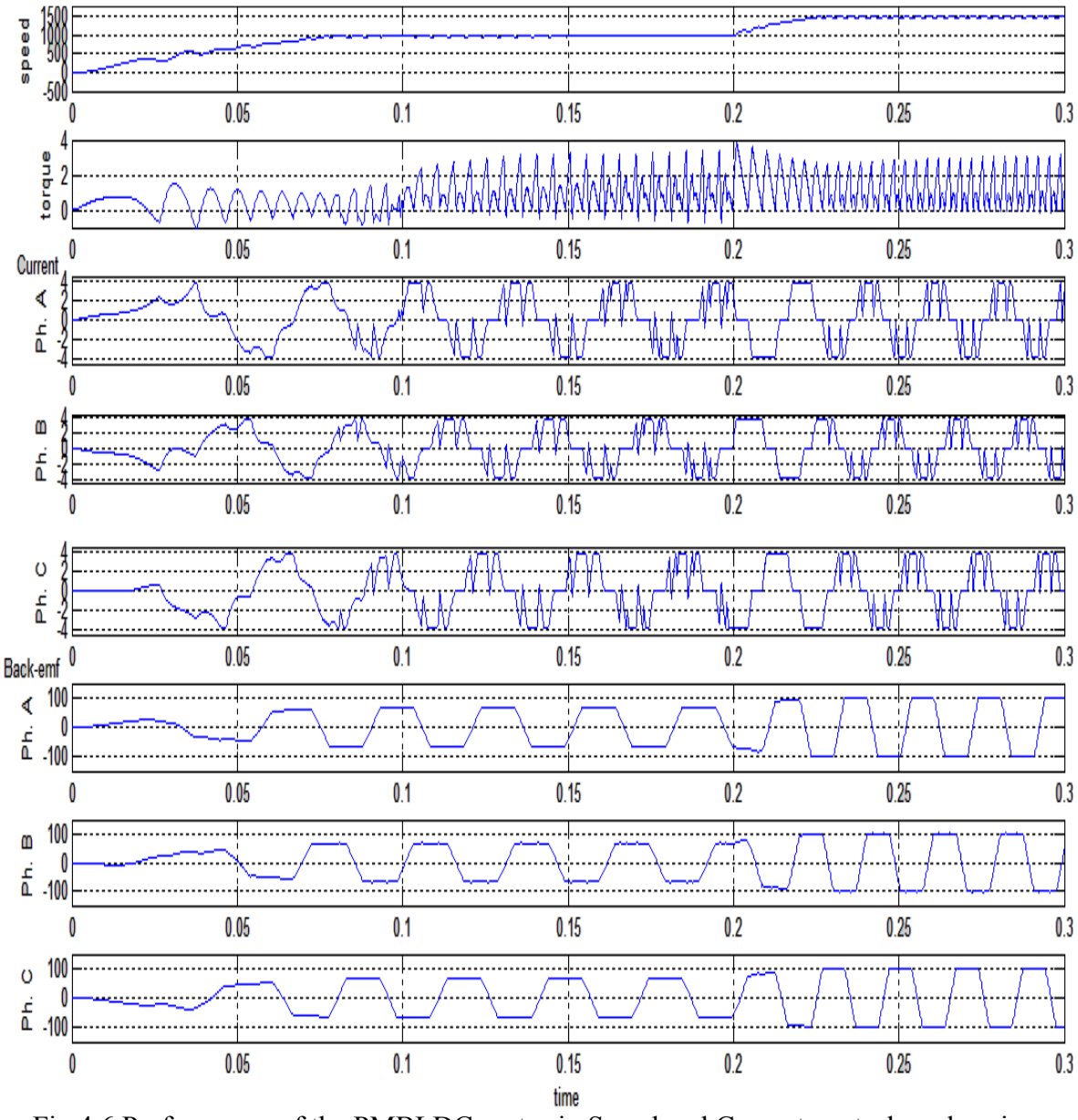

Fig 4.6 Performance of the PMBLDC motor in Speed and Current control mode using Speed sensor only

From the speed performance in figure 4.6 it is observed that the motor takes about 0.0817 seconds to reach the initial reference speed of 1000 Rpm. Also the sudden application of the load of 1 Nm at 0.1 seconds on the motor did not cause a noticeable dip in motor speed. When the reference speed is changed to 1500 Rpm at instant t=0.2 seconds, no overshoot in speed is observed and motor takes 0.0285 sec. to reach reference of 850 Rpm.

From the torque response, it is observed at instant 0.2seconds, when there is change in reference speed; the electromagnetic torque rises to a value 3.584Nm. Also here the starting torque produced is 1.466 Nm.

It is observed from the current performance that the starting current drawn by the motor is 2.136A. During the load perturbation i.e. at the instant 0.1 seconds at which a sudden load of 1Nm is applied on motor shaft, the value of current is increased compared to the no-load current. After the load is applied the motor is drawing a current of 3.829 A. The current drawn by the motor is also much closer to the rectangular shape but large variation in its magnitude. It is observed that when the reference speed is changed from 1000 RPM to 1500 RPM then there is only a large overshoot in the current values, from 3.829A to 3.852A. There is a small change in the value of current as the current controller does not allow sudden large variation and current error is permitted only to 0.01A. Here also, the current behavior is similar to the rectangular one and the fluctuation is little less.

From back-emf waveform it is observed that it increases with the increasing speed and becomes constant when the speed is constant. Also at time, t=0.2 seconds when the speed increases then correspondingly back-emf also increases. It means follow the relation that back-emf is directly proportional to speed.

4.2.2.3 Simulation result of PMBLDCM in Speed and Current Control mode (At low speed)

Fig. 4.7 show the performance of the PMBLDC motor drive with PI speed controller (K_p=2 and K_i=0.8) and current hysteresis controller when only speed sensor is used. The motor is running at the reference speed of 700 RPM up to 0.2 seconds which is then changed to 850 RPM.

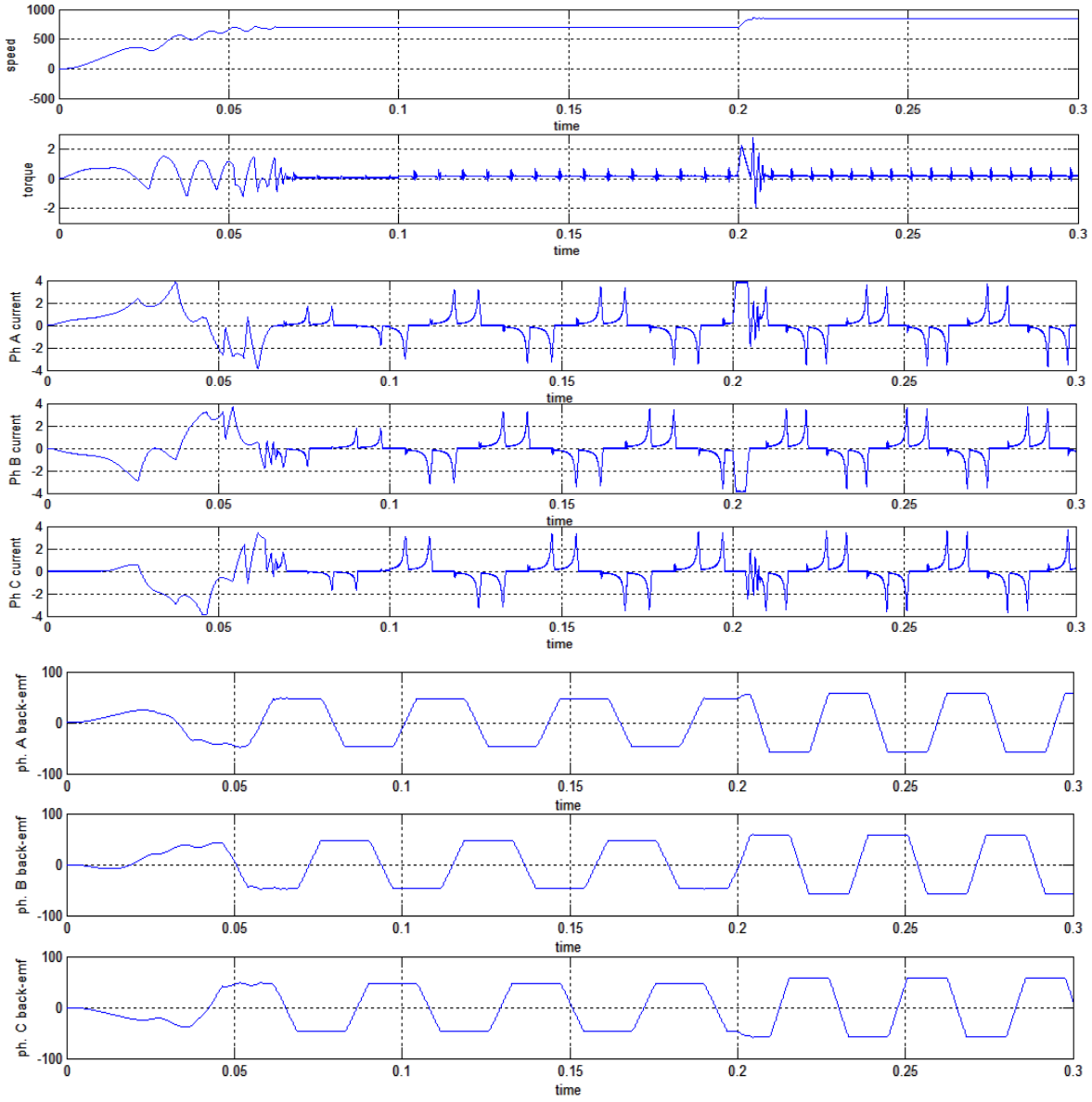

Fig 4.7 Performance of the PMBLDC motor in Speed and Current control mode using Speed sensor only (Low speed operation)

From the speed performance in figure 4.7 it is observed that the motor takes about 0.0636 seconds to reach the initial reference speed of 700 Rpm. Also the sudden application of the load of 0.1 Nm at 0.1 seconds on the motor did not cause a noticeable dip in motor speed. When the reference speed is changed to 850 Rpm at instant t=0.2 seconds, no overshoot in speed is observed and the motor reaches the reference speed of 850 Rpm in 0.005 seconds. From the torque response, it is observed at instant 0.2seconds, when there is change in reference speed; the electromagnetic torque rises to a value 2.487 Nm. Also here the starting torque produced is 1.469 Nm.

It is observed from the current performance that the starting current drawn by the motor is 2.303A. During the load perturbation i.e. at the instant 0.1 seconds at which a sudden load of 1Nm is applied on motor shaft, the value of current is increased compared to the no-load current. After the load is applied the motor is drawing a current of 3.137 A. The current drawn by the motor is also much closer to the rectangular shape but large variation in its magnitude. It is observed that when the reference speed is changed from 1000 RPM to 1500 RPM then there is only a large overshoot in the current values, from 3.137A to 3.859A. There is a small change in the value of current as the current controller does not allow sudden large variation and current error is permitted only to 0.01A. Here also, the current behavior is similar to the rectangular one and the fluctuation is little less.

From back-emf waveform it is observed that it increases with the increasing speed and becomes constant when the speed is constant. Also at time, t=0.2 seconds when the speed increases then correspondingly back-emf also increases. It means follow the relation that back-emf is directly proportional to speed.

4.3 SENSORLESS OPERATION OF PMBLDCM

4.3.1 Back-Emf and Speed Controller based Operation of PMBLDCM

4.3.1.1 Simulation result of PMBLDCM in Speed control mode with 120 degree commutation

Fig. 4.8 show the performance of the PMBLDC motor drive with PI speed controller (K_p= 0.8 and K_i=0.0007) and simultaneously observing the polarity of back-emf waveform to carry out the commutation. Here the polarity of back-emf wave is observed for every 120 degree. The motor is running at the reference speed of 1000 RPM up to 0.2 seconds which is then changed to 1500 RPM.

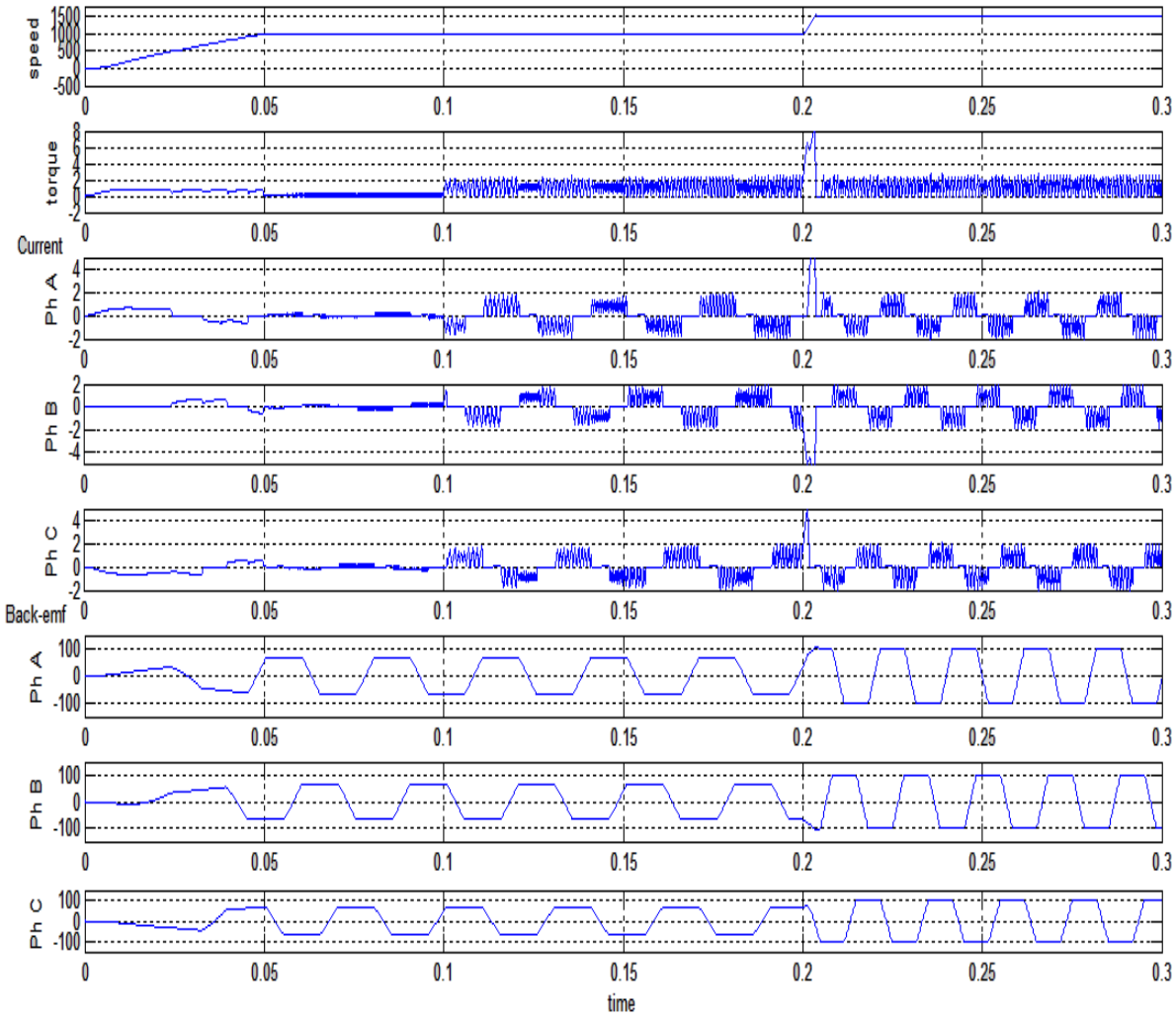

Fig 4.8 Performance of the PMBLDC motor in speed control mode using 120 degree commutation with no sensor

From the speed performance in figure 4.8 it is observed that the motor takes about 0.04994 seconds to reach the initial reference speed of 1000 Rpm. Also the sudden application of the load of 1 Nm at 0.1 seconds on the motor did not cause a noticeable dip in motor speed. When the reference speed is changed to 1500 Rpm at instant t=0.2 seconds, then a small overshoot of 46 Rpm in speed can be observed.

From the torque response, it is observed that when the load is applied, there are large ripples in torque as there is no control over the current and torque depends on it and also at instant when there is change in reference speed, the electromagnetic torque suddenly rises to a value about 8.082Nm. Also here the starting torque produced is approx. 0.8102Nm.

It is observed from the current performance that the starting current drawn by the motor is 0.5955A. During the load perturbation i.e. at the instant 0.1 seconds at which a sudden load of 1Nm is applied on motor shaft, the value of current is increased compared to the no-load current. After the load is applied the motor is drawing a current of 1.82 A. The current drawn by the motor is also much closer to the rectangular shape but large variation in its magnitude. It is observed that when the reference speed is changed from 1000 RPM to 1500 RPM then there is only a large overshoot in the current values, from 1.82A to 6.145A. This is due to absence of current controller which could otherwise limit this value. Here also, the current behavior is similar to the rectangular one but the fluctuation is also large. The current conduction takes for every 120 degree and commutation for next 60 degree.

From back-emf waveform it is observed that it increases with the increasing speed and becomes constant when the speed is constant. Also at time, t=0.2 seconds when the speed increases then correspondingly back-emf also increases. It means follow the relation that back-emf is directly proportional to speed.

4.3.1.2 Simulation result of PMBLDCM in Speed control mode with 180 degree commutation

Fig. 4.9 show the performance of the PMBLDC motor drive with PI speed controller (K_p= 1.5 and K_i=0.8) and simultaneously observing the polarity of back-emf waveform to carry out the commutation. Here the polarity of back-emf wave is observed for every 180 degree. The motor is running at the reference speed of 1000 RPM up to 0.2 seconds which is then changed to 1500 RPM.

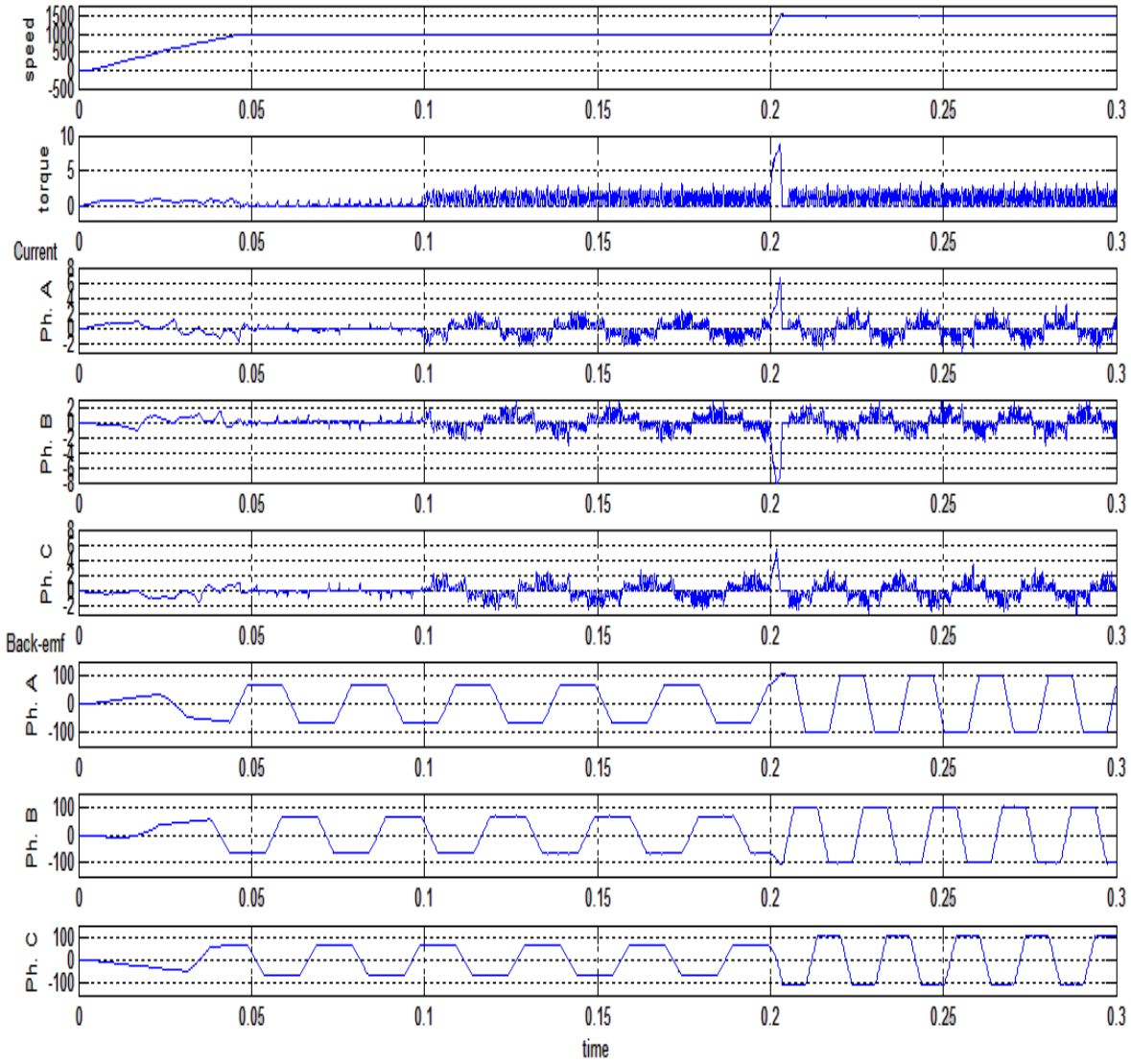

Fig 4.9 Performance of the PMBLDC motor in speed control mode using 180 degree commutation with no sensor

From the speed performance in figure 4.9 it is observed that the motor takes about 0.04534 seconds to reach the initial reference speed of 1000 Rpm. Also the sudden application of the load of 1 Nm at 0.1 seconds on the motor did not cause a noticeable dip in motor speed. When the reference speed is changed to 1500 Rpm at instant t=0.2 seconds, then a overshoot is observed.

From the torque response, it is observed that when the load is applied, there are large ripples in torque as there is no control over the current and torque depends on it and also at instant when there is change in reference speed, the electromagnetic torque suddenly rises to a value about 8.856Nm. Also here the starting torque produced is approx. 1.096Nmwhich is larger than the staring torque produced in 120 degree commutation scheme. It is observed from the current performance that the starting current drawn by the motor is about 1.185A. During the load perturbation i.e. at the instant 0.1 seconds at which a sudden load of 1Nm is applied on motor shaft, the value of current is increased compared to the no-load current to about 2.224 A. It is observed that the phase of the sensorless 180-degree commutation conducts current in each conduction intervals. The stator terminal connects to either the positive or the negative of the dc power supply, which results in no back-EMF appeared at the stator terminals. It is also observed that when the reference speed is changed from 1000 RPM to 1500 RPM then there is a large overshoot in the current values, from 2.224 A to 6.562 A. One reason for drawing a large current is the mode of operation without current controller. Another reason for the motor to take larger current than the current drawn in 120 degree commutation scheme is that the three stator resistances are allocated as one is in series with the parallel connection of the other two resistors in 180 degree so the overall phase to phase resistance is less than the value of 120-degree. That is why the phase current of 180-degree is larger than that of 120-degree commutation under the same power supply voltage, which results in more power is delivered from inverter side to the motor side.

From back-emf waveform it is observed that it increases with the increasing speed and becomes constant when the speed is constant. Also at time, t=0.2 seconds when the speed increases then correspondingly back-emf also increases. It means follow the relation that back-emf is directly proportional to speed.

4.3.2 Simulation result of PMBLDCM in Speed and Current Control Mode

Fig. 4.10 show the performance of the PMBLDC motor drive with PI speed controller (K_p= 1.5 and K_i=0.8) and current hysteresis controller when NO sensor is used. The motor is running at the reference speed of 700 RPM up to 0.2 seconds which is then changed to 900 RPM. The Hysteresis band width for the current controller is 0.02A.

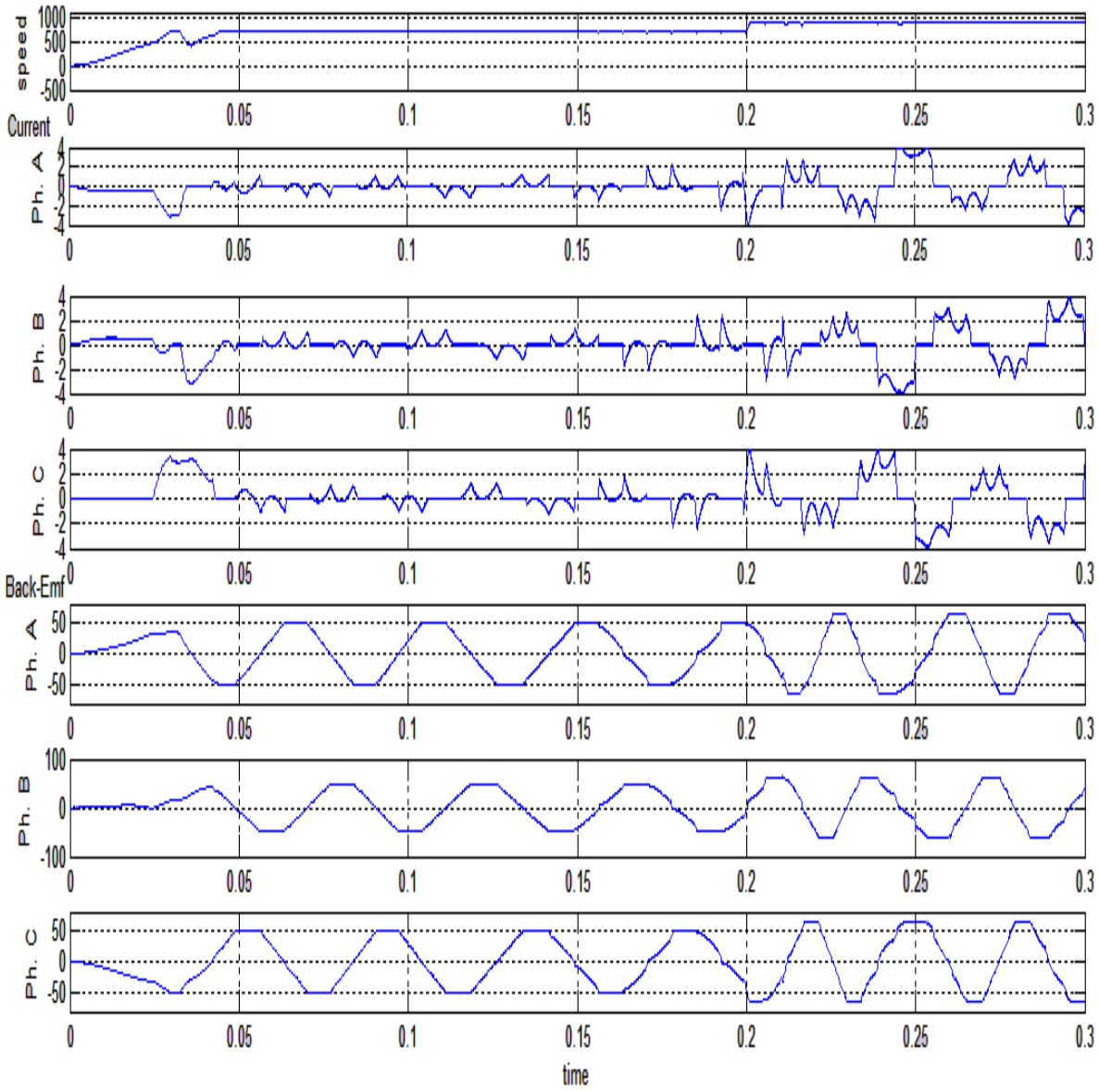

Fig 4.10 Performance of the PMBLDC motor drive in speed and current control mode using NO SENSOR

From the speed performance in figure 4.10 it is observed that the motor takes about 0.04432 seconds to reach the initial reference speed of 700 Rpm. Also the sudden application of the load of 0.3 Nm at 0.1 seconds on the motor did not cause a noticeable dip in motor speed. When the reference speed is changed to 900 Rpm at instant t=0.2 seconds, no overshoot in speed is observed and the motor reaches the reference speed of 900 Rpm at 0.2016 seconds time.

It is observed from the current performance that the starting current drawn by the motor is about 1.011 A. During the load perturbation i.e. at the instant 0.1 seconds at which a sudden load of 0.3 Nm is applied on motor shaft, the value of current is increased compared to the no-load current to about 1.139 A. The current drawn by the motor is closer to the rectangular shape but large dips in its magnitude. It is observed that when the reference speed is changed from 700 RPM to 900 RPM then there is only a large overshoot in the current values, from about 1.139A to 3.702 A and then settles to about 2.5 A.

Back-emf waveform in fig. 4.9 is obtained from the line voltage difference. The back-emf is increasing with the increasing speed and becomes constant when the speed is constant. Also at time, t=0.2 seconds when the speed increases then correspondingly back-emf also increases. It means it follows the relation that back-emf is directly proportional to speed.

4.4 FUZZY LOGIC CONTROLLER BASED SPEED AND CURRENT CONTROL OF PMBLDCM USING SPEED SENSOR

Fig. 4.11 show the performance of the PMBLDC motor drive with Fuzzy Logic speed controller and current hysteresis controller using Speed encoder sensor is used. The motor is running at the reference speed of 700 RPM up to 0.2 seconds which is then changed to 850 RPM. Here the same scheme as in the topic 4.2.2.3. The only difference is in the speed controller.

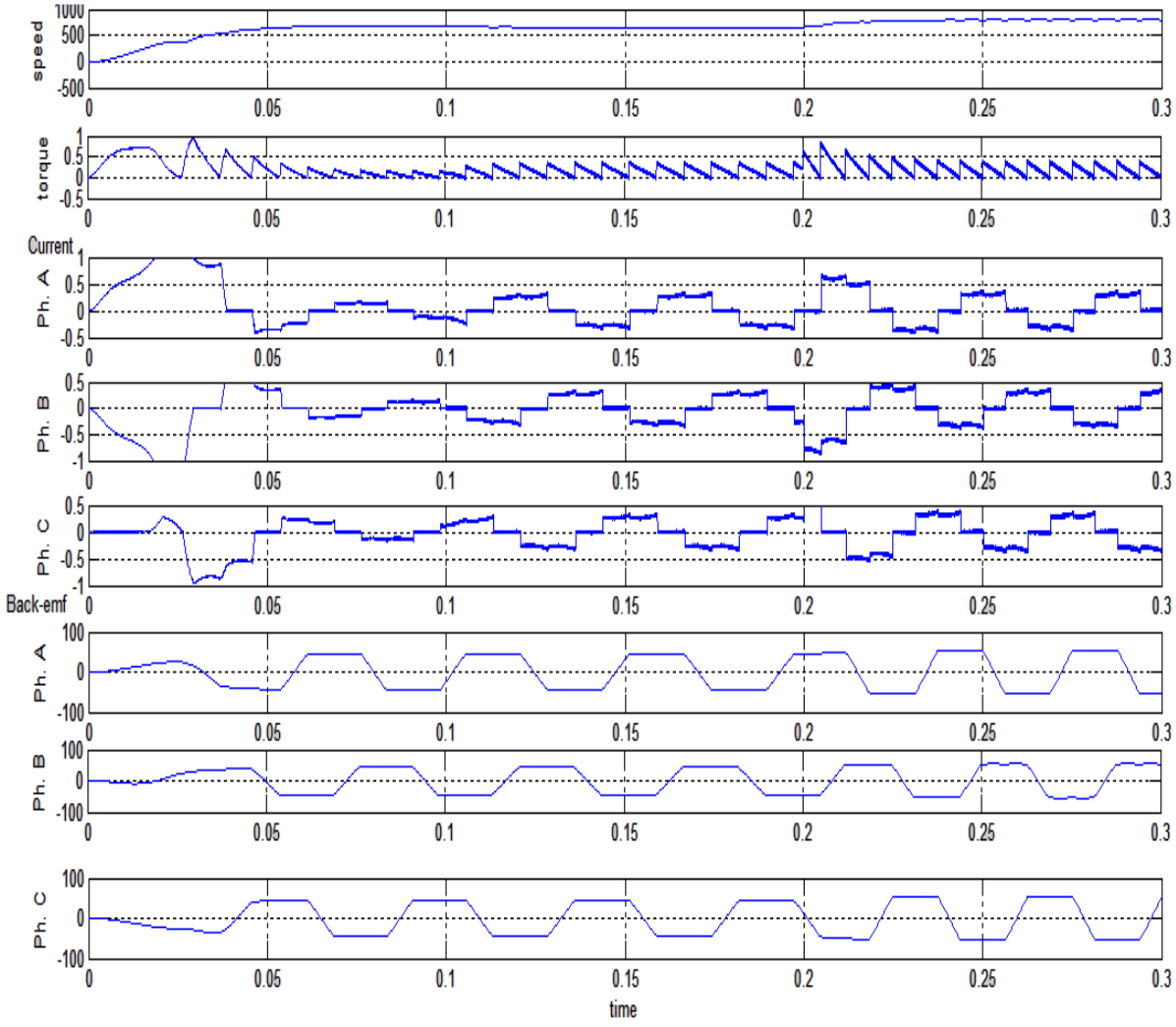

Fig 4.11 Performance of the PMBLDC motor in Speed and Current control mode using Speed Sensor and FLC

From the speed performance in figure 4.11 it is observed that the motor takes about 0.05737 seconds to reach the initial reference speed of 700 Rpm. Also the sudden application of the load of 0.1 Nm at 0.1 seconds on the motor did not cause a noticeable dip in motor speed. When the reference speed is changed to 850 Rpm at instant t=0.2 seconds, no overshoot is observed and reaches the target in 0.027 seconds.

From the torque response, it is observed that when the load is applied, there are large ripples in torque as there is no control over the current and torque depends on it and also at instant when there is change in reference speed, the electromagnetic torque suddenly rises to a value 0.8256Nm. Also here the starting torque produced is 0.948Nm.

It is observed from the current performance that the starting current drawn by the motor is 0.9348A. During the load perturbation i.e. at the instant 0.1 seconds at which a sudden load of 1Nm is applied on motor shaft, the value of current is increased compared to the no-load current. After the load is applied the motor is drawing a current of 0.3075 A. The current drawn by the motor is also much closer to the rectangular shape but large variation in its magnitude. It is observed that when the reference speed is changed from 1000 RPM to 1500 RPM then there is only a large overshoot in the current values, from 0.3075A to 0.93A. This value of current is very high and close to the current rating. This is due to absence of current controller which could otherwise limit this value. Here also, the current behavior is similar to the rectangular one but the fluctuation is also large.

From back-emf waveform it is observed that it increases with the increasing speed and becomes constant when the speed is constant. Also at time, t=0.2 seconds when the speed increases then correspondingly back-emf also increases. It means follow the relation that back-emf is directly proportional to speed.

CONCLUSION

The Simulation and performance evaluation of PM brushless DC motor in various modes operation is done in this chapter. The commutation of PMBLDC motor is done using sensors and without sensors. The performance is analyzed in terms of torque ripple, magnitude of current drawn, smooth operation and dynamic response. It is observed from the simulated results that mode of operation using both the speed and current controller not only limit the current in the windings and makes the operation of PMBLDCM smooth and efficient but also improve the torque ripples correspondingly in comparison to its performance with the mode of operation using only speed controller. The current controller also keeps the current in the windings near to the rectangular shape which along with the trapezoidal back-emf produces unidirectional torque. The torque produced by the motor is a reflection of the current so less the current ripple; less will be the torque ripple. In the sensorless mode of operation also, good performance in terms of torque ripple, dynamic response in terms of rise time and current shape and amount drawn by the motor is observed. In the mode of operation using the Fuzzy logic speed controller better performance is observed in comparison to the mode using the PI speed controller.

CHAPTER V

MAIN CONCLUSION AND FUTURE SCOPE OF WORK

5.0 MAIN CONCLUSION

The present work was motivated to evaluate the performance of the Permanent Magnet Brushless DC Motor in different modes of operation using Matlab/Simulink software.

A detailed study of the Permanent Magnet motors, their classifications, properties, advantages, earlier motors trends and their drawbacks is carried out. A detailed literature survey and summary of important development in the area of PM machines during last few decades is briefly described.

A detailed study on both kinds of Permanent Magnet Motors i.e. PM Synchronous Motors and PM Brushless DC Motors is presented.

The PMBLDC motor is also called inverted DC motor in terms of position of armature winding and field circuit. As in DC motor mechanical commutation is carried with the help of brushes and commutator, here in PMBLDC motor commutation is carried electronically. Commutation is simply the reversal of current in windings so as to produce the unidirectional torque on the motor. But due to the mechanical wear and tear, DC motors efficiency gets poor so electronic commutation is done in BLDC motors. During the electronic commutation, the switching of phases is done so as to produce the desirable unidirectional torque.

A thorough study of all the important components needed for the power and control circuit of PMBLDC motors has also been described like AC-to-DC Rectifier, Capacitor Filter, Boost Regulator, three Phase inverter etc.

In this dissertation, the performance of Permanent Magnet Brushless DC motor is evaluated under various modes like open loop mode and closed loop mode. Another category for performance evaluation of the PMBLDC motor is in terms of controlled parameters. Some schemes are modeled and simulated for only the speed control of the PMBLDC motor and some are modeled and simulated for the speed as well as current control. Then there is another categorization of the mode, based on the thing whether the use of sensors has been made or not. In some models, sensors are used and sensorless

scheme also been modeled and simulated. Initially the electronic commutation is performed using the three Hall Effect Sensors which are employed on the stator body and 120 degrees apart. Though the Hall Effect sensors produce less torque ripples and current harmonics but the performance characteristics of motor employed with sensors would get degrade while working in the oily, dusty and sluggish environment. Later, the trapezoidal back-emf of the PMBLDC motor is used to identify the position of rotor but the estimation of back-emf is difficult. In order to simplify the commutation process, later, one position/speed encoder is used. Here also results are good but still the problem is same with the use of sensors. The next purpose of the work is to make the electronic commutation of the PMBLDC motor without hall sensors and speed senor. Here the line voltages which can be easily measured, is used to get the back-emf of the motor which can further be processed to get the speed/position of the rotor.

A complete study of the BLDC motor and its controlling strategies has imparted a fairly good knowledge in the PM machines in terms of their performance in different modes of operation.

5.1 FUTURE SCOPE OF THE WORK

Here in the dissertation, only PI and hysteresis current controller is being used for the controlling process. In one scheme it has been shown that Fuzzy Logic Speed Controller has improved the performance of the PMBLDC motor in comparison to its performance with the PI speed controller. With recent developments of the semiconductor devices and high speed digital processes i.e. microcontroller and DSP, the implementation of advanced adaptive controllers are possible with advance capabilities and features in modern drives. The performance of the PMBLDC motor with such advance controllers may further enhance the quality of the work.

****

APPENDIX

PMBLDC Motor Specification

3.2 Nm, Vn drive540 V, 3000 Rpm

Sr. No.	Parameter	Value
1	Poles Number	4
2	Voltage Constant ±5% (V/krpm)	136.1357
3	Torque Constant ±5% (Nm/A)	1.3
4	Stall Current (A)	2.46
5	Peak Torque (Nm)	9.60
6	Peak Current (A)	7.4
7	Max Current (A)	8.6
8	Resistance/phase (Ω)	10.91
9	Inductance/Phase (mH)	30.01
10	Insulation Class	F
11	Moment of inertia (kgcm^2)	2.9
12	Mechanical Time Constant (ms)	1.4/1.8

References

[1] Pragasan Pillay and R. Krishnan, “Modeling, Simulation, and Analysis of Permanent Magnet Motor Drives, Part I: The Permanent-Magnet Synchronous Motor Drive," *IEEE Transactions on Industry Applications*, Vol. 25, no. 2, pp.265-273, March-April 1989.

[2] R. Krishnan, “Control and Operation of PM Synchronous motor drives in the field - weakening region,” pp. 745-750, IEEE 1993.

[3] Pragasan Pillay and R. Krishnan,“Modeling of Permanent Magnet Motor Drives”, in *IEEE Trans. on Industrial Electronics*, vol. 35, no. 4, pp. 537-541, November 1988.

[4] Javad Soleimani, Abolfazal Vahedi, “3 Phase Surface Mounted PMSM improvement considering Hard Magnetic Material Type,” at *International Journal of Advanced Engineering Sciences and Technologies,* vol. No. 7, Issue No. 1, 036 – 041.

[5] Salih Baris Ozturk Bilal Akin Hamid A. Toliyat Farhad Ashrafzadeh, "Low-Cost Direct Torque Control of Permanent Magnet Synchronous Motor Using Hall-Effect Sensors" pp.667-673, IEEE 2006.

[6] Badre Bossoufi, Mohammed Karim, Ahmed Lagrioui, Badre Bossoufi, Silviu Ioniţă ," Performance Analysis of Direct Torque Control (DTC) for Synchronous Machine Permanent Magnet (PMSM*)," 2010 IEEE 16th International Symposium for Design and Technology in Electronic Packaging (SIITME)*,pp. 242,23-26 Sept 2010,Pitesti, Romania, IEEE,2010.

[7] G. Foo and M.F. Rahman,"An Extended Rotor-Flux Model for Sensorless Direct Torque and Flux Control of Interior Permanent-Magnet Synchronous Motor Drives,"

ELECTROMOTION 2009 – EPE Chapter 'Electric Drives' Joint Symposium, France, IEEE July 2009.

[8] Gilbert Foo and M. F. Rahman, "A Novel Speed Sensorless Direct Torque and Flux Controlled Interior Permanent Magnet Synchronous Motor Drive" pp. 50-56 IEEE, 2008.

[9] Lang Baohua, Yang Jianhua, Liu Weiguo "Research on Space Vector Modulation Method for Improving the Torque Ripple of Direct Torque Control," *International Conference On Computer Design And Appliations (ICCDA 2010)*,vol 3,pp. 502-506, 2010.

[10] Bhim Singh, B.P. Singh and Sanjeet Dwivedi, "DSP Based Implementation of Sliding Mode Speed Controller for Direct Torque Controlled PMSM Drive," pp.1301-1308, IEEE 2006.

[11] M. B. B. Sharifian, T. Herizchi and K. G. Firouzjah, "Field Oriented Control of Permanent Magnet Synchronous Motor Using Predictive Space Vector Modulation," *IEEE Symposium on Industrial Electronics and Applications (ISIEA 2009),* pp.574-579,October 2009, Malaysia.

[12] Ji Hua, Zibo, Li Zhiyong, "Simulation of Sensorless Permanent Magnetic Brushless DC Motor Control System" *Proceedings of the IEEE International Conference on Automation and Logistics Qingdao*, pp. 2847-2851, September 2008.

[13] Vinatha U, Swetha Pola, , Dr K.P.Vittal," Simulation of Four Quadrant Operation & Speed Control of BLDC Motor on MATLAB / Simulink", *TENCON,* pp.1-6, IEEE 2008.

[14] Pragasan Pillay and R. Krishnan,"Modeling Simulation and Analysis of Permanent Magnet Motor Drives, Part II: The Brushless DC Motor Drives", in *IEEE Trans. on Industrial Applications*, vol. 25, no. 2, pp. 274-279, March/April 1989.

[15] Nicola Bianchi, Silverio Bolognani, Ji-Hoon Jang, and Seung-Ki Sul, "Comparison of PM Motor Structures and Sensorless Control Techniques for Zero-Speed Rotor Position Detection" in *IEEE Trans. on Power Electronics*, vol. 22, no. 6, pp. 2466-2475, November 2007.

[16] Yoseph Buchnik and Rad Rabinovici," Speed and Position Estimation of Brushless Dc Motor In Very Low speeds", pp-317-320, IEEE 2004.

[17] Balogh Tibor, Viliam Fedák, František Ďurovský, "Modeling and Simulation of the BLDC Motor in MATLAB GUI", pp. 1403-1407, IEEE 2011.

[18] R. Somanatham, P. V. N. Prasad, A. D. Rajkumar," Modeling and Simulation of Sensorless Control of PMBLDC Motor Using Zero-Crossing Back E.M.F Detection", *SPEEDAM 2006 International Symposium on Power Electronics, Electrical Drives, Automation and Motion,*pp-S4-24-S4-29.

[19] Boyang–Hu and Swamidoss Sathia Kumar, "Sensorless drive of Permanent Magnet Brushless DC motors with 180 degree commutation," at *IEEE Conference on Robotics, Automation and Mechatronics*, pp. 106-111, 2010 IEEE.

[20] Y. S. Jeon, H. S. Mok, G. H. Choe, D. K. Kim, J. S. Ryu, "*A New Simulation Model of BLDC Motor With Real Back EMF Waveform*", pp-217-220, IEEE 2000.

[21] Somesh Vinayak Tewari, B.Indu Rani, " Torque Ripple Minimization of BLDC Motor with un-ideal Back EMF", *Second International Conference on Emerging Trends in Engineering and Technology, ICETET-09*,pp-687-690.

[22] K. S. Rama Rao, Nagadeven and Soib Taib, "Sensorless Control of a BLDC Motor with Back EMF Detection Method using DSPIC", *2nd IEEE International Conference on Power and Energy (PECon 08)*, pp-243-248 IEEE December 2008.

[23] Jianwen Shao, "An Improved Microcontroller-Based Sensorless Brushless DC (BLDC) Motor Drive for Automotive Applications", *IEEE Trans. on Industry Application,* vol. 42, no. 5, pp. 1216-1221 September/October 2006.

[24] Wook-Jin Lee and Seung-Ki Sul and Seung-Ki Sul ,"A New Starting Method of BLDC Motors without Position Sensor",*39th Industry Applications Conference*, vol. 4, pp 2397-2402, IEEE 2004.

[25] Yen-Shin Lai, Senior Member, IEEE, and Yong-Kai Lin, "Novel Back-EMF Detection Technique of Brushless DC Motor Drives for Wide Range Control Without Using Current and Position Sensors " *IEEE TRANS. on Power Electronics,* vol. 23, no. 2,pp. 934-940, March 2008.

[26] J. X. Shen, Q. Zhu, Senior, and David Howe, "Sensorless Flux-Weakening Control of Permanent-Magnet Brushless Machines Using Third Harmonic Back EMF",*IEEE Trans. on Industry Application*, vol. 40, no. 6, pp. 1629-1636, November/December 2004.

[27] J. X. Shen, and S. Iwasaki "Sensorless Control of Ultrahigh-Speed PM Brushless Motor Using PLL and Third Harmonic Back EMF", *IEEE Trans. on Industrial Electronics*, vol. 53, no. 2, pp. 421-428, April 2006.

[28] Maher Faeq, Dahaman Ishak ," A new Scheme Sensorless Control of BLDC Motor Using Software PLL and Third Harmonic Back-EMF*", 2009 IEEE Symposium on*

Industrial Electronics and Applications (ISIEA 2009), Kuala Lumpur, Malaysia,pp-861-865, IEEE October 2009.

[29] Kuang-Yao Cheng, Member, IEEE, and Ying-Yu Tzou, Member, IEEE." Design of a Sensorless Commutation IC for BLDC Motors" *IEEE Transactions on Power Electronics,* vol. 18, no. 6, pp.-1365-1375, November 2003.

[30] A. Ungurean, V. Coroban-Schramel and I. Boldea," Sensorless control of a BLDC PM motor based on I-f starting and Back-EMF zero-crossing detection" *2010, 12th International Conference on Optimization of Electrical and Electronic Equipment, OPTIM ,* pp.-377-382, 2010.

[31] Alin Ştirban, Ion Boldea, Fellow, IEEE, Gheorghe-Daniel Andreescu, Senior Member, IEEE, Dorin Iles, Member, IEEE, and Frede Blaabjerg, Fellow, IEEE, "Motion Sensorless Control of BLDC PM Motor with Offline FEM Info Assisted State Observer",*2010, 12th International Conference on Optimization of Electrical and Electronic Equipment, OPTIM,* pp.-321-328, 2010.

[32] Yuanyuan Wu, Zhiquan Deng, Xiaolin Wang, Xing Ling, and Xin Cao, " Position Sensorless Control Based on Coordinate Transformation for Brushless DC Motor Drives", *IEEE Transactions on Power Electronics,* vol. 25, no. 9, pp.-2365-2371, September 2010.

[33] Paul P. Acarnley and John F. Watson, "Review of Position-Sensorless Operation of Brushless Permanent-Magnet Machines", *IEEE Trans. on Industrial Electronics,* vol. 53, no. 2, pp. 352-362, April 2006.

[34] P. Damodharan and Krishna Vasudevan, Member, IEEE, "Sensorless Brushless DC Motor Drive Based on the Zero-Crossing Detection of Back Electromotive Force

(EMF) From the Line Voltage Difference" *IEEE Transactions On Energy Conversion, vol. 25, no. 3,* pp-662-668, September 2010.

[35] Carlo Concari Fabrizio Troni, "Sensorless Control of BLDC Motors at Low Speed Based on Differential BEMF Measurement", pp.-1772-1777, IEEE 2010.

[36] Satoshi Ogasawara and Hirofumi Akagi, "An Approach to Position Sensorless Drive for Brushless dc Motors", *IEEE Transactions on Industry Applications,* vol. 27, no. 5*,* pp-928-933, September-October 1991.

[37] E. Kaliappan,C. Chellamuthu, "A Simple Sensorless Control technique for PMBLDC Motor Using Back EMF Zero Crossing" *European Journal of Scientific Research ISSN 1450-216X* , vol.60 no.3, pp.365-378, 2011.

[38] Fernando Briz, Michael W. Degner, Pablo García, and Robert D. Lorenz, "Comparison of Saliency-Based Sensorless Control Techniques for AC Machines", *IEEE Trans. on Industry Application*, vol. 40, no. 4, pp. 1107-1115, July/August 2004.

[39] Ajay Kumar Bansal, R. A. Gupta, , and Rajesh Kumar," Fuzzy estimator for Sensorless PMBLDC Motor Drive under Speed Reversal," *India International Conference on Power Electronics (IICPE)*, pp.1-7, IEEE 2011

[40] A. Albert Rajan and Dr. S. Vasantharathna "Fuzzy Logic Based Reconfigurable Optimal Switching Controller for BLDC Motor for Reduced Harmonics" at *IPEC*, pp. 578-583, IEEE 2010.

[41] Atef Saleh Othman Al-Mashakbeh , "Proportional Integral and Derivative Control of Brushless DC Motor*", European Journal of Scientific Research ISSN 1450-216X,* vol.35 no.2 (2009), pp.198-203.

[42] Tribeni Prasad Banerjee, Joydeb Roy choudhury, Swagatam Das, and Ajith Abraham," Hybrid Intelligent Predictive Control System for High Speed BLDC Motor in Aerospace Application", *Third International Conference on Emerging Trends in Engineering and Technology*, pp.-258-262.

[43] G. H. Jang, J. H. Park and J. H. Chang, " Position detection and start-up algorithm of a rotor in a sensorless BLDC motor utilizing inductance variation" *IEE Proceeding online no 20020022,*pp.137-142, 2002.